

Revision 1

1 **AMFORM, a new mass-based model for the calculation of the unit formula of amphiboles from**  
2 **Electron Micro-Probe analyses**

3 **FILIPPO RIDOLFI<sup>1\*</sup>, ALBERTO ZANETTI<sup>2</sup>, ALBERTO RENZULLI<sup>3</sup>, DIEGO PERUGINI<sup>4</sup>, FRANCOIS**  
4 **HOLTZ<sup>1</sup>, ROBERTA OBERTI<sup>2</sup>**

5 <sup>1</sup>Institut für Mineralogie, Leibniz Universität Hannover, 30167 Hannover, Germany

6 <sup>2</sup>CNR-Istituto di Geoscienze e Georisorse, Sede secondaria di Pavia, 27100 Pavia, Italy

7 <sup>3</sup>Dipartimento di Scienze Pure e Applicate, Università degli Studi di Urbino “Carlo Bo”, 61029 Urbino,  
8 Italy

9 <sup>4</sup>Dipartimento di Fisica e Geologia, Università di Perugia, 06100 Perugia, Italy

10

11

**ABSTRACT**

12 In this work, we have studied the relationships between mass concentration and unit-formula of  
13 amphibole using 114 carefully selected high-quality experimental data, obtained by EMP (Electron  
14 Micro-Probe) + SREF (Single-crystal X-ray Structure REFinement) ± SIMS (Secondary-Ion Mass  
15 Spectrometry) analyses, of natural and synthetic Li-free monoclinic species belonging to the Ca and  
16 Na-Ca subgroups, and 75 Li-free and Mn-free *C2/m* end-members including oxo analogues of Ca  
17 amphiboles. Theoretical considerations and crystal-chemical driven regression analysis allowed us to  
18 obtain a number of equations which can be used to: (i) calculate from EMP analyses amphibole unit-  
19 formulae consistent with SREF±SIMS data, (ii) discard unreliable EMP analyses and (iii) estimate  
20 <sup>W</sup>O<sup>2-</sup> and Fe<sup>3+</sup> contents in Li-free *C2/m* amphiboles with relatively low Cl contents (≤1 wt%). The  
21 AMFORM approach mostly relies on the fact that while the cation mass in Cl-poor amphiboles

Revision 1

22 increases with the content of heavy elements, its anion mass maintains a nearly constant value, i.e.,  
23  $22O + 2(OH, F, O)$ , resulting in a very well-defined polynomial correlation between the molecular  
24 mass and the cation mass per gram ( $R^2 = 0.998$ ).

25 The precision of estimating the amphibole formula (e.g.,  ${}^T\text{Si} \pm 0.02$ ,  ${}^C\text{Al} \pm 0.02$ ,  ${}^A(\text{Ca} + \text{Na} + \text{K}) \pm 0.04$  apfu)  
26 is 2-4 times higher than when using methods published following the last IMA recommended scheme  
27 (2012). It is worth noting that most methods using IMA1997 recommendations (e.g., PROBE-AMPH)  
28 give errors which are about twice those of IMA2012-based methods. A linear relation between  ${}^W\text{O}^{2-}$   
29 and the sum of  ${}^C(\text{Ti}, \text{Fe}^{3+})$  and  ${}^A(\text{Na} + \text{K})$  contents, useful to estimate the iron oxidation state of highly-  
30 oxidized amphiboles typical of post-magmatic processes, is also proposed. A step by step procedure  
31 (Appendix 1) and a user-friendly spreadsheet (AMFORM.xlsx, provided as supplementary material)  
32 allowing one to calculate amphibole unit-formulae from EMP analyses are presented. This work opens  
33 new perspectives on the unit-formula calculation of other minerals containing OH and structural  
34 vacancies (e.g., micas).

35 **Keywords:** Li-free amphiboles, oxo component, cation mass, amphibole oxidation, amphibole  
36 deprotonation, SREF, SIMS, Mössbauer spectroscopy

37  
38 *Corresponding author:* [filippo.ridolfi@uniurb.it](mailto:filippo.ridolfi@uniurb.it)

39

40

## INTRODUCTION

41 Amphiboles are a supergroup of silicate minerals containing, either at the major- or at the trace-element  
42 level, most elements of geological/geochemical relevance (for a review, see Hawthorne et al. 2007). It  
43 has been largely recognized that the role of amphibole in understanding geological/planetary processes

Revision 1

44 and several health issues is of crucial importance (e.g., Forbes and Starmer 1974; Foley et al. 2002;  
45 Gunter et al. 2007; McCanta et al. 2008; Jackson et al. 2013; Smith 2014). Amphibole crystal-  
46 chemistry has captured the attention of many scientists over the years because of its intrinsic  
47 complexity (indeed, the term amphibole derives from the Greek “αμφιβολος”, which means  
48 ambiguous; Haiÿy 1801; see also Cipriani et al. 2007) and its ability to record the steps of a wide range  
49 of geochemical and petrological processes due to a network of mutual relationships between cation  
50 ordering, chemistry of the associated phases (minerals and/or melt) and intrinsic parameters such as  
51 pressure, temperature and fugacity of volatile elements (Hammarstrom and Zen 1986; Holland and  
52 Blundy 1994; Al’meev et al. 2002; Oberti et al. 2000, 2007a; Ridolfi et al. 2010; Ridolfi and Renzulli  
53 2012; Zhang et al. 2017). However, the prerequisite for using amphiboles as geological markers is the  
54 determination of their correct crystal-chemical formula (i.e., composition and site partitioning).

55 In the 70s and 80s, amphibole unit-formula calculation was a hot topic in the geological community  
56 (e.g., Stout 1972; Smith 1977; Leake 1978; Laird and Albee 1981; Hawthorne 1983; Rock and Leake  
57 1984; Spear and Kimball 1984; Jacobson and Sorensen 1986) which has led to two major  
58 recommended schemes of the International Mineralogical Association (IMA; Leake et al. 1997;  
59 Hawthorne et al. 2012). Routine calculations of amphibole unit-formulae from electron microprobe  
60 (EMP) data may be seriously affected by inappropriate normalization procedures and/or the lack of  
61 accurate information on the oxidation state of iron and the contents of hydrogen and lithium (Leake et  
62 al. 1997; Al’meev et al. 2002; Hawthorne et al. 2012; Locock 2014). In particular, most of the  
63 published schemes for formula calculation do not account for the occurrence of  $O^{2-}$  as W anion (e.g.,  
64 Tindle and Webb 1994; Leake et al. 1997; Al’meev et al. 2002; Esawi 2004; Dale et al. 2005) which  
65 allows the number of total negative (and positive) charges to theoretically vary between 46 and 48  
66 (Hawthorne et al. 2012). The spreadsheet of Locock (2014) can only account for a maximum content of  
67  $O^{2-}$  in the W- sites ( ${}^W O^{2-}$ ) equal to 2 times the total content of Ti in C, thus disregarding the

Revision 1

68 contribution of the oxidation of Fe to balance deprotonation. This lack of information leads to poorly  
69 constrained cation contents (mainly cation underestimations) and  $\text{Fe}^{3+}/\text{Fe}_{\text{tot}}$  estimates which, at the best,  
70 are averages between the maximum and minimum values (e.g., Leake et al. 1997). Nevertheless, there  
71 is a large amount of amphibole literature data reporting H,  $^{\text{W}}\text{O}^{2-}$  and  $\text{Fe}^{3+}/\text{Fe}_{\text{tot}}$  measurements and/or  
72 accurate estimates (e.g., Robinson et al. 1997; Bottazzi et al. 1999; Oberti et al. 2000; Tiepolo et al.  
73 2003; Adam et al. 2007; Oberti et al. 2007b; Uvarova et al. 2007; Perinelli et al. 2012; Della Ventura et  
74 al. 2014) that can be used to improve the existing methods to calculate amphibole unit-formulae.

75 In this work, we use high-quality literature data and end-member compositions to analyze the  
76 relation between elemental concentration (by mass) and stoichiometry in the amphibole supergroup and  
77 propose a new mass-based method to be applied only to EMP data, that allows identification of bad  
78 analyses and calculation of the correct unit-formula of Li-free (and Mn- and Cl-poor) *C2/m*  
79 amphiboles, with an uncertainty 2-4 times lower than that of recently published procedures (i.e.,  
80 Hawthorne et al. 2012; Locock 2014). Tests of the most used formula calculation methods (Tindle and  
81 Webb 1994; Dale et al. 2005; Locock 2014) are also provided as supplementary material.

82

### 83 **ESSENTIAL DEFINITIONS**

84 Amphibole supergroup has the general formula  $\text{A}_{0-1}\text{B}_2\text{C}_5\text{T}_8\text{O}_{22}\text{W}_2$  (Hawthorne et al. 2012). The  
85 amphiboles considered in this work are Li- and  $\text{Mn}^{3+}$ -free *C2/m* species and their group elements  
86 include: A = Na, K, Ca, □ (vacancy); B = Ca, Na,  $\text{Mn}^{2+}$ ,  $\text{Fe}^{2+}$ , Mg; C = Mg, Ti,  $\text{Fe}^{2+}$ ,  $\text{Mn}^{2+}$ , Cr, Ni, Zn,  
87 Al,  $\text{Fe}^{3+}$ ; T = Si, Al, Ti; W =  $\text{OH}^-$ , F, Cl,  $\text{O}^{2-}$  (where Mn, Cr, Ni, Zn and Cl are minor components, ≤  
88 0.2 atoms per formula unit, apfu). Site-assignments and stoichiometric constraints for these amphiboles  
89 are provided in Table 1 while Table 2 reports the ideal formula and composition of 75 end-members.

Revision 1

90 Definitions needed to follow the text are provided below. Note that most of the calculations needed  
91 to obtain the defined parameters are reported in Appendix 1.

92 - *original composition*: concentrations expressed as wt% of the oxides (SiO<sub>2</sub>, TiO<sub>2</sub>, Al<sub>2</sub>O<sub>3</sub>, Cr<sub>2</sub>O<sub>3</sub>,  
93 FeO<sub>tot</sub>, NiO, ZnO, MnO, MgO, CaO, Na<sub>2</sub>O, K<sub>2</sub>O) and halogens (F, Cl) in the amphibole,  
94 usually measured by EMP analyses;

95 - *TEO: Total Elements and Oxides* (also named re-calculated total), wt% sum of oxides (see  
96 previous definition) and halogens (F, Cl), minus FeO<sub>tot</sub> (total iron content) and the oxygen  
97 atoms balancing F and Cl (i.e., O<sup>F,Cl</sup>), plus Fe<sub>2</sub>O<sub>3</sub>, FeO and H<sub>2</sub>O calculated from the unit-  
98 formula (Appendix 1), where calculated H<sub>2</sub>O values correspond to those measured by  
99 Secondary-Ion Mass Spectrometry (hereafter SIMS) or estimated by Single-crystal X-ray  
100 Structure REFinement (hereafter SREF) by published equations relating the oxo component to  
101 the *M*(1)-*M*(2) distance (Oberti et al. 2007a; see following section and Supplement 1 for  
102 methods). Note that *TEO* values from original compositions generally deviate from ideality  
103 (100 wt%);

104 - *normalized composition*: concentrations expressed as wt% of the oxides and halogens (F, Cl) in  
105 amphibole calculated from any unit-formula to obtain a value of *TEO* equal to 100 wt% (e.g.,  
106 Table 1 and <http://webmineral.com> for end-members);

107 - *M<sub>r</sub> (g/mol)*: molecular mass corresponding to the sum of the apfu of all elements (Table 1)  
108 previously multiplied by their atomic mass (*A<sub>r</sub>*), ;

109 - *cmpg*: cation mass per gram, i.e.,  $cmpg = 10^{-2}(\text{Si} + \text{Ti} + \text{Al} + \text{Cr} + \text{Fe} + \text{Ni} + \text{Zn} + \text{Mn} + \text{Mg} +$   
110  $\text{Ca} + \text{Na} + \text{K})$ , calculated from the original or normalized compositions, all elements in wt%  
111 (see Appendix 1 for calculation). Note that *cmpg* is a mass ratio and it thus corresponds to the  
112 total cation mass divided by the sum of the total cation and anion masses for normalized  
113 compositions;

Revision 1

- 114 -  $X_i$ : mass of element  $i$  divided by the total cation mass (see Appendix 1). Note that  $X_i$  values are  
115 the same in normalized and original compositions;
- 116 -  $^Yi$ : element or ion  $i$  in a generic group-sites  $Y$ , where  $Y$  can be T, C, B, A and W (Table 1).  
117 When superscript is not reported,  $i$  refers to the total amount of  $i$  in amphibole. To avoid  
118 misunderstanding the total amount of iron is expressed as  $Fe_{tot}$  (e.g., Table 1);
- 119 -  $CR$  ( $apfu \cdot g/mmole$ ): correlation ratio between the sums of the  $apfu$  and  $mmole/g$  (millimole per  
120 gram) of all cation components, i.e.  $CR = \frac{\sum_{Si \rightarrow K} Si \text{ } apfu}{\sum_{Si \rightarrow K} \frac{mmole}{g}}$  (Table 1). Note that  $CR$  is ideally equal  
121 to the  $apfu \cdot g/mmole$  value of any cation (e.g.,  $CR^{Si} = \frac{Si \text{ } apfu}{Si \text{ } mmole/g}$ ) or anion (e.g.,  $CR^F =$   
122  $\frac{F \text{ } apfu}{F \text{ } mmole/g}$ ). Once precisely determined (see below), it can be easily used to calculate the  $apfu$  of  
123 each element multiplying  $CR$  by the element concentration in  $mmole/g$  (see Appendix 1);
- 124 -  $\Delta charge$ : deviation from electroneutrality in an amphibole unit-formula (i.e., positive – negative  
125 charge sums);
- 126 -  $dC$  and  $dB$ : deviation from 5  $apfu$  and 2  $apfu$  in the C- and B-group cations in the selected unit-  
127 formulae, not admitted by the stoichiometric constraints (Table 1; see also section Selection  
128 criteria of the calibration dataset);
- 129 -  $\Delta C$ : the amount of  $Fe^{2+}$ , Mn and/or Mg exceeding 5  $apfu$  and thus considered as B-group  
130 cations in the calculated formula (Table 1; Appendix 1).

131

132

## DATA SELECTION AND TECHNIQUES

### 133 Composition and petrogenesis of the investigated amphiboles

Revision 1

134 We have studied the relationships between concentration and unit-formula in Li-free and Mn, Cl-poor  
135 monoclinic amphiboles belonging to the Ca, Na-Ca subgroups (and some of their oxo analogues) using  
136 a dataset carefully selected from the literature and from the CNR-IGG (Consiglio Nazionale delle  
137 Ricerche-Istituto di Geoscienze e Georisorse) amphibole database available in Pavia; selection was  
138 done based on the availability of accurate EMP+SREF±SIMS analyses. The dataset contains 114  
139 oxides-formula pairs with the largest possible geochemical and geological variability; the oxo-  
140 amphiboles considered are kaersutite, ferri-kaersutite, oxo-potassic-chromio-katophorite, oxo-potassic-  
141 taramite, Ti-rich oxo-sadanagaite, Ti-rich oxo-pargasite and Ti-rich oxo-ferri-pargasite (see  
142 AMFORM.xlsx in the supplementary material). Compositions belonging to the sodium amphiboles  
143 were excluded because they may contain minor to moderate amounts of Li (e.g., Hawthorne et al.  
144 1993) which cannot be detected and measured by EMP analysis.

145 The dataset includes published concentration (wt%)-formula (apfu) pairs of both 61 synthetic  
146 (Oberti et al. 2000; Bottazzi et al. 1999; Tiepolo et al. 2000; 2003; Adam et al. 2007) and natural  
147 amphiboles which are typical of geologically relevant systems (gabbro, peridotite, lherzolite, kyanite-  
148 eclogite, marble, metasomatic/skarn-type deposit and several types of metavolcanic amphibolites) and  
149 coming from different world-wide localities (Oberti et al. 1995; Vannucci et al. 1995; Robinson et al.  
150 1997; Oberti et al. 2007b; 2015; Uvarova et al. 2007; Perinelli et al. 2012; Della Ventura et al. 2014).  
151 53 unpublished oxides-formula pairs come from the CNR-IGG database and include amphiboles from  
152 extrusive rocks, mantle ultramafic rocks (hornblendites, pyroxenites, peridotites), peridotitic and  
153 pegmatitic veins (for a list, cf. AMFORM.xlsx).

154

### 155 **Sample characterization**

156 All the unpublished amphiboles had been analyzed by EMP, SREF and SIMS allowing a complete  
157 characterization of their crystal-chemical parameters (AMFORM.xlsx). SREF and SIMS analyses were

Revision 1

158 done at CNR-IGG in Pavia, while EMP analyses were mostly done at the University of Manitoba  
159 (Winnipeg, Canada). See electronic supplement 1 for a more detailed information on the CNR-IGG  
160 analytical methods. The crystal-chemical formulae were calculated by combining SREF, EMP and  
161 SIMS results. The number of A-cations was estimated on the basis of the refined site-scattering values  
162 at the relevant sites and the K<sub>2</sub>O and Na<sub>2</sub>O contents from EMP analysis. The oxo component was  
163 evaluated either by SIMS or by a SIMS-calibrated crystal-chemical relationship (Oberti et al. 2007a;  
164 see also electronic supplement 1). Under these constraints, the Fe<sup>3+</sup> content can be derived based on the  
165 overall electroneutrality. The Fe<sup>3+</sup> content and its distribution were further constrained through the  
166 pattern of refined mean bond-lengths observed at the three *M*(1-3) octahedra. The presence of the *M*(4')  
167 subsite, indicating the occurrence of small B cations (i.e., Mn<sup>2+</sup>, Fe<sup>2+</sup>, Mg), was checked on the  
168 difference Fourier maps. B cations were calculated assigning excess C cations (i.e., ΔC, first Mn<sup>2+</sup> and  
169 then Fe<sup>2+</sup> and Mg) trying to minimize the difference between the site scattering calculated (from EMP)  
170 for the B and C cations and those obtained by SREF. For further validation, the <sup>T</sup>Al contents obtained  
171 by recalculation of EMP analyses was checked to be in close agreement with those calculated from the  
172 refined <*T*(1)-O> and <*T*(2)-O> distances (Oberti et al. 2007a).

173 Many of the amphiboles taken from the literature include EMP, SREF and SIMS data, and their  
174 formulae were obtained following the same procedure. The amphibole formula selected from Robinson  
175 et al. (1997) was derived from EMP, SREF, Mössbauer spectroscopy (for Fe<sup>3+</sup>/Fe<sub>tot</sub>), wet-chemical (for  
176 F) and IR (InfraRed spectroscopy, for H<sub>2</sub>O) analyses. In some cases, the formulae were derived from  
177 the only EMP and SREF data (Oberti et al. 1995; Vannucci et al. 1995; Oberti et al. 2007b; Della  
178 Ventura et al. 2014), and the oxo component was estimated using the correlation developed at CNR-  
179 IGG in Pavia based on SREF results (Oberti et al. 2007a). In other cases, the Fe<sup>3+</sup> content of the  
180 amphibole was validated by Mössbauer spectroscopy (Uvarova et al. 2007, Perinelli et al. 2012). For



Revision 1

181 the oldest selected data (Oberti et al. 1995) the occurrence of  $^{18}\text{O}^{2-}$  in amphibole was estimated during  
182 this work using the published SREF data (see above).

183

#### 184 **Selection criteria of the calibration dataset**

185 Both literature and unpublished analyses were checked according to a series of criteria aimed at  
186 obtaining a high-quality dataset.

187 Whenever standard deviations (oxide  $\sigma$ ) of the EMP element oxide analyses are available  
188 together with averaged compositions, we discarded amphibole data showing oxide  $\sigma$  values higher than  
189 2/3 of the average oxide  $\sigma$  values reported by Ridolfi and Renzulli (2012) for their high-quality  
190 experimental amphibole compositions. We also discarded the amphibole compositions with *TEO*  
191 values falling outside the range of  $100 \pm 1.7$  wt%, because larger deviations from 100 wt% may derive  
192 from analytical problems for some elements, resulting in error propagation to the unit-formula. The  
193 amphibole compositions in the dataset have *TEO* values ranging from 98.3 to 100.8 wt%.

194 Amphibole formulae showing  $\Delta$ charge larger than  $\pm 0.05$ , *dC* and *dB* larger than  $\pm 0.01$  and/or  
195 total cation apfu (i.e.,  $\sum \text{Si} \rightarrow \text{K}$ ; Table 1) higher than 16.005 were also discarded. In addition, formulae  
196 calculated without considering the oxo component, i.e., forcing the negative charges to be 46, were not  
197 considered. The bijection between the composition and formula of any amphibole was carefully  
198 checked comparing the *CR* values of each of the major elements (e.g.,  $CR^{\text{Si}}$ ,  $CR^{\text{Al}}$ ,  $CR^{\text{Mg}}$ ) with the *CR*  
199 value calculated on the total cation sum ( $\sum \text{Si} \rightarrow \text{K}$ ; Appendix 1). This procedure allowed us to avoid  
200 mismatches between formulae and compositions due to adjustment and/or editing.

201 The dataset used to calibrate the method contains 114 entries and it is included in the  
202 AMFORM.xlsx spreadsheet (provided as supplementary material). The ranges in elemental  
203 composition are:  $^{\text{T}}\text{Si} = 5.8\text{-}7.8$  apfu;  $^{\text{A}}(\text{Ca}+\text{Na}+\text{K}) = 0.1\text{-}1.0$  apfu;  $^{\text{W}}\text{F} \leq 1.3$  apfu;  $^{\text{W}}\text{Cl} \leq 0.2$  apfu;  
204  $\text{Mg}/(\text{Mg}+\text{Fe}^{2+}) = 0.2\text{-}1.0$ ;  $\text{Fe}^{3+}/\text{Fe}_{\text{tot}} = 0.0\text{-}1.0$ .

Revision 1

205 It is worth noting that oxides-formula pairs not validated by SREF were not included in this  
206 final calibration dataset. This decision was taken to guarantee an independent check of the formulae  
207 and a reliable constraint on  $\sum\text{Si}\rightarrow\text{K}$  values.

208 Beside the 114 selected amphibole compositions, for calibration we used 75 ideal formulae and  
209 (normalized) compositions of Li- and Mn-free *C2/m* end-members of the amphibole supergroup  
210 (Hawthorne et al. 2012) (Table 2). The oxides-formula pairs in Table 1 also include kaersutite, ferri-  
211 kaersutite, ferro-kaersutite, ferro-ferri-kaersutite and some oxo analogues of the Ca groups as these  
212 amphiboles in nature may often have a significant oxo-component.

213

## 214 **RATIONALE AND DATA ANALYSES**

215 The high-quality dataset described above was used to detect and analyze any possible relation between  
216 compositional (e.g., wt% and *mmol/g*) and unit-formula parameters (apfu) in amphiboles.

217 For a correct characterization of the amphibole unit-formula, two crucial parameters must be  
218 determined:  $\sum\text{Si}\rightarrow\text{K}$ , ranging from 15 to 16 apfu and the oxo component ( $^{\text{W}}\text{O}^{2-}$ ; 0-2 apfu), which  
219 allows the sum of the negative charges to vary between 46 and 48 (Table 1). When these parameters  
220 are known and the presence of  $\text{Mn}^{3+}$  can be excluded, the amount of  $\text{Fe}^{3+}$  can be derived under the  
221 constraint of electroneutrality (Hawthorne et al. 2012).

222

### 223 **Development of the CR-equations**

224 The correlation ratio (*CR*) between apfu and *mmol/g* of any component or sum of components (e.g., Si;  
225  $\text{Fe}_{\text{tot}}$ , F;  $\sum\text{Si}\rightarrow\text{K}$ ) must be constant for any normalized and end-member composition-formula pair. If

Revision 1

226 *CR* is known with a reasonably good approximation, the apfu content of each element can be calculated  
227 multiplying *CR* by its concentration in *mmol/g*.

228 Figure 1a shows that the *CR* of the normalized and end-member compositions is perfectly  
229 correlated with their molecular mass,  $M_r$ :

$$230 \quad CR = 10^{-3} M_r \left( \text{apfu} \cdot \frac{\text{g}}{\text{mmol}} \right) \quad (R^2 = 1.000) \quad (1)$$

231 Indeed, equation (1) is an identity because *CR* is mathematically equal to  $M_r$  divided 1000 for  
232 the ideal composition of any mineral and compound. The original amphibole compositions only  
233 slightly deviate from this linear trend (blue symbols in Fig. 1a). The deviations are due to *TEO* values  
234 usually lower than 100% (see above). However, this simple correlation cannot be used to estimate *CR*  
235 from EMP analysis because  $M_r$  can only be calculated from the formula. Indeed, equation (1) should be  
236 used at the end of any formula calculation procedure to calculate *CR* after  $M_r$  has been calculated from  
237 the formula, thus validating the final results and the quality of the data (see below).

238 Figure 1b shows that the *CR* values of normalized and end-member compositions have a nearly  
239 perfect polynomial relation with the cation mass per gram (*cmpg*) which can be directly calculated  
240 from EMP data (see above):

$$241 \quad CR = 4.809 \text{cmpg}^2 - 3.409 \text{cmpg} + 1.276 \quad (\text{apfu} \cdot \text{g}/\text{mmol}) \quad (R^2 = 0.998) \quad (2)$$

242 Indeed, the anion components in the different amphibole compositions have almost the same  
243 mass, because they mostly consist of the same number of ions with similar  $A_r$ , i.e.,  $22\text{O}^{2-} + 2(\text{OH}^-, \text{F}^-,$   
244  $\text{O}^{2-})$ . In contrast, the mass of the cation component increases with the amount of heavier cations (e.g.,  
245  $\text{Fe}^{2+}, \text{Fe}^{3+}$ ) resulting in a progressively increasing pattern of *CR* (and  $M_r$ ) with *cmpg*. Because *cmpg* is a  
246 mass ratio, Figure 1b has a curvilinear trend. The small scattering observed for some normalized and  
247 end-member compositions ( $R^2 = 0.998$ ; Fig. 1b) is due to the occurrence of  $^{\text{W}}(\text{Cl}^-, \text{F}^-, \text{O}^{2-})$  which have  
248  $A_r$  values different from that of  $\text{OH}^-$ , thus affecting the *cmpg* values. For example, the heaviest end-  
249 member ferro-ferri-cannilloite has the same cation mass as its oxo analogue but a higher  $M_r$  value

Revision 1

250 because it differs (in mass term) by having two more hydrogen atoms (Table 2). Therefore, the mass of  
251 W anions is higher than that of its oxo equivalent (because  $\text{OH}^-$  is heavier than  $\text{O}^{2-}$ ) resulting in a *cmpg*  
252 value slightly lower than that of oxo-ferro-ferri-cannilloite (Fig. 1b; Table 1). F-rich amphiboles  
253 behave in the opposite way because  $\text{F}^-$  has a mass higher than  $\text{OH}^-$ . However the effect of  $\text{F}^-$  and  $^{\text{W}}\text{O}^{2-}$   
254 in calculating *CR* is minimal as confirmed by the high determination coefficient ( $R^2$ ) of equation 2  
255 (Fig. 1b), so that amphibole compositions with high F and oxo contents can be treated with this method  
256 with a sufficient accuracy.

257 In contrast, amphiboles with high Cl contents (e.g., Léger et al. 1996; Coogan et al. 2001)  
258 deviate significantly from equation 2 (towards lower *cmpg*) because the  $A_r$  value of chlorine is about  
259 twice that of F, OH and O. However, the maximum Cl content (i.e., 0.20 apfu, corresponding to 0.72  
260 wt%) in the high-quality dataset produces negligible deviations from equation 2. This is because the  
261 incorporation of Cl in amphibole is always related to high  $\text{Fe}^{2+}$  contents (e.g., Oberti et al. 2007a)  
262 which results in relatively low *cmpg* underestimations (e.g., in the two Fe- and Cl-rich amphiboles  
263 marked with green triangles in Fig. 1b).

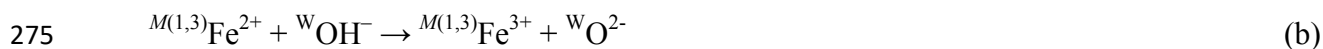
264 It is worth noting that equation 2 cannot be successfully applied to the original compositions of  
265 most of the amphiboles because EMP uncertainties commonly result in incorrect *CR* and *cmpg* values  
266 leading to significant deviations from the normalized composition, i.e., from total elements and oxides  
267 equal to 100 wt% (Fig. 1b). Therefore, at least a preliminary estimation of  $^{\text{W}}\text{O}^{2-}$ ,  $\text{H}_2\text{O}$  and *TEO*,  
268 followed by a normalization calculation of the original composition, is required.

269

## 270 **The oxo component, $^{\text{W}}\text{O}^{2-}$**

271 It is commonly accepted that  $^{\text{W}}\text{O}^{2-}$  and  $^{\text{W}}\text{OH}^-$  contents in amphibole mostly depend on two substitution  
272 mechanisms involving cations occurring at the *M*(1) and *M*(3) sites (e.g., King et al. 1999; Popp et al.  
273 2006; Oberti et al. 2007a):

Revision 1



276 During igneous and metamorphic processes, the OH<sup>-</sup> content of amphibole is mostly ruled by  
277 substitution mechanism (a) wherein the amount of OH<sup>-</sup> at the W site is reduced by twice the amount of  
278 Ti incorporated at the M(1) site. Substitution (a) mostly occurs at high-T low-*f*H<sub>2</sub>O conditions, and  
279 involves chemical exchange of major components such as Mg, Fe<sup>2+</sup> and Ti with the surrounding  
280 environment (i.e., minerals and melt). During magma ascent or hydrothermal alteration, amphibole  
281 may undergo a high T-*f*O<sub>2</sub> process of deprotonation (i.e., dehydrogenation) involving iron oxidation  
282 according to substitution mechanism (b).

283 From a crystal-chemical viewpoint, the occurrence of <sup>W</sup>O<sup>2-</sup> induces important changes in the  
284 cation-ordering scheme typical of amphiboles, where high-charged C cations are fully ordered at the  
285 M(2) site, with the only exception of Al, which may disorder between the M(2) and M(3) sites in high-  
286 T Mg-rich pargasites and edenites (Oberti et al. 1995; Della Ventura et al. 2014). The different bond-  
287 valence bond-strength requirements of the O(3) oxygen after H<sup>+</sup> loss must be satisfied by the presence  
288 of high-charged cations at the coordinated M(1) (with multiplicity 2) and M(3) sites. This feature of the  
289 amphibole solid-solution system implies complex but strongly related compositional changes that can  
290 be empirically discerned using multivariate least-square analysis (e.g., Ridolfi and Renzulli 2012;  
291 Ridolfi et al. 2014; Zhang et al. 2017).

292 Among the 114 amphiboles in the calibration dataset, 87 formulae have <sup>W</sup>O<sup>2-</sup> ≤ 2<sup>C</sup>Ti implying  
293 that mechanism (b) is almost not or weakly active. Hereafter, for these amphiboles we will use the  
294 prefix “poorly-oxidized” to remind that the amount of <sup>M(1,3)</sup>Fe<sup>3+</sup> due to post-crystallization oxidation is  
295 zero or very low. These amphiboles may contain up to 1.3 apfu <sup>W</sup>O<sup>2-</sup>, which mostly derives from  
296 mechanism (a). However, the constraint of all the Ti in C-group cations (<sup>C</sup>Ti) as a proxy for the oxo  
297 component (Hawthorne et al. 2012; Locock 2014) may be severely misleading because in these

Revision 1

298 samples a significant amount of  ${}^C\text{Ti}$  is often ordered at the  $M(2)$  site and hence does not contribute to  
299 mechanism (a) (Oberti et al. 2007a).

300 Regression analysis shows that the  ${}^W\text{O}^{2-}$  content in poorly-oxidized amphiboles (with  ${}^W\text{O}^{2-} \leq$   
301  $2{}^C\text{Ti}$ ) can be estimated with reasonably low errors (Fig. 2a) using the following equation:

$$\begin{aligned} 302 \quad {}^W\text{O}^{2-} = & -6.684X_{Si} + 11.025X_{Ti} - 0.989X_{Al} - 2.800X_{Fetot} - 20.359X_{Mn} - 0.903X_{Mg} - \\ 303 \quad & 6.875X_{Ca} - 11.119X_{Na} - 2.553X_K + 5.751X_F + 4.610 \text{ apfu} \end{aligned} \quad (3)$$

304 This equation can be applied without any previous calculation of the amphibole formula, as it only  
305 depends on the values of the cation fractions ( $X_i$ ) calculated from EMP analyses. In addition, the  $X_i$   
306 values are the same in both original and normalized compositions because a generalized overestimation  
307 (or underestimation) does not change the mass ratios.

308 A drawback of equation 3 is that it underestimates  ${}^W\text{O}^{2-}$  in highly-oxidized amphiboles (where  
309  ${}^W\text{O}^{2-} > 2{}^C\text{Ti}$ ), which underwent high-T, high- $f\text{O}_2$  post-magmatic and/or hydrothermal alteration  
310 according to the mechanism (b). However, this issue may even turn out to be an advantage when  
311 studying the processes of magmatic crystallization from amphibole crystals which underwent post-  
312 magmatic oxidation-deprotonation.  $f\text{O}_2$  in high-T magmatic environments (up to  $\sim 10^{-7}$  bar,  
313 corresponding to a  $\log f\text{O}_2$  of 3-4 units above the Ni-NiO buffer, hereafter NNO; Ridolfi and Renzulli  
314 2012) is several orders of magnitude lower than in air ( $\sim 0.21$  bar, i.e.,  $-0.68 \log f\text{O}_2$ ; Namur et al. 2012)  
315 where high-T post-magmatic oxidation most probably occurs. It is worth noting that the highly-  
316 oxidized amphiboles in our calibration dataset are Ca-dominant megacrysts (rapidly ejected to the  
317 surface from high T-P conditions) or mantle amphiboles crystallized from hydrothermal fluids (e.g.  
318 late-stage veins in peridotites, metasomatic deposits).

319 At this point, we analyzed correlations between the measured values of  ${}^W\text{O}^{2-}$  and cation  
320 compositional parameters in both poorly and highly oxidized amphiboles, starting from the assumption  
321 that the fractions of Ti and  $\text{Fe}^{3+}$  occurring at the  $M(1)$  and  $M(3)$  sites are directly involved in the

Revision 1

322 process of deprotonation. The best correlation we found for the 114 amphiboles in the dataset is  
323 reported in Figure 2b: i.e.,  ${}^W\text{O}^{2-} = 0.963[4/3{}^C\text{Ti} + 2/3{}^C\text{Fe}^{3+} + 2/3{}^A(\text{Na}+\text{K})] - 0.624$ . The overall  
324 correlation shows a reasonably good  $R^2$  value (0.927) and closely approaches the equation:

$$325 \quad {}^W\text{O}^{2-} = 4/3{}^C\text{Ti} + 2/3{}^C\text{Fe}^{3+} + 2/3{}^A(\text{Na}+\text{K}) - 2/3 \text{ apfu} \quad (4a)$$

326 Equation 4a works well both for poorly ( ${}^W\text{O}^{2-} \leq 2{}^C\text{Ti}$ ) and highly ( ${}^W\text{O}^{2-} > 2{}^C\text{Ti}$ ) oxidized amphiboles  
327 when  $4/3{}^C\text{Ti} + 2/3{}^C\text{Fe}^{3+} + 2/3{}^A(\text{Na}+\text{K})$  is  $\geq 2/3$ . At those values, the only two samples significantly  
328 deviating from equation 4a (giving a  ${}^W\text{O}^{2-}$  overestimation up to 0.49 apfu) are rare Na-Ca amphiboles,  
329 i.e., alumino-taramite K22-2 and fluoro-alumino-magnesio-taramite DJ102-23, which are characterized  
330 by high  ${}^C\text{Fe}^{3+}$  and A-cation contents but, according to their crystal-chemical characterization do not  
331 contain oxo component (Oberti et al. 2007b; Fig. 2b). In Figure 2b, amphiboles with  $4/3{}^C\text{Ti} + 2/3{}^C\text{Fe}^{3+}$   
332  $+ 2/3{}^A(\text{Na}+\text{K}) \leq 2/3$  have zero or negligible  ${}^W\text{O}^{2-}$  contents, providing the constraint:

$$333 \quad {}^W\text{O}^{2-} = 0 \text{ apfu, if } 4/3{}^C\text{Ti} + 2/3{}^C\text{Fe}^{3+} + 2/3{}^A(\text{Na}+\text{K}) \leq 2/3 \text{ apfu} \quad (4b)$$

334 When applying equations 4a and constraint 4b we obtain a  $\sigma_{\text{est}} = 0.12$  apfu for the whole dataset (Fig.  
335 2b). When the two major outliers alumino-taramite K22-2 and fluoro-alumino-magnesio-taramite  
336 DJ102-23 are not considered, the maximum error decreases from 0.49 to 0.3 apfu which is even lower  
337 than that indicated by equation 3 for only the poorly-oxidized amphiboles (0.4 apfu; Fig. 2a).

338 Equation (4a) and constraint (4b) can be easily applied to any amphibole unit-formula anytime  
339 an independent measurement of  $\text{Fe}^{3+}/\text{Fe}_{\text{tot}}$  is available. When this is not the case,  ${}^W\text{O}^{2-}$  and  $\text{Fe}^{3+}$   
340 contents can be estimated using a system of two linear equations including (4a) and the charge balance  
341 equation:

$$342 \quad 4(\text{Si}+\text{Ti}) + 3(\text{Al}+\text{Cr}+\text{Fe}^{3+}) + 2[\text{Mg}+(\text{Fe}_{\text{tot}}-\text{Fe}^{3+})+\text{Mn}+\text{Ni}+\text{Zn}+\text{Ca}] + \text{Na}+\text{K} = 46 + {}^W\text{O}^{2-} \quad (4c)$$

343 where the uncertainty of the  ${}^W\text{O}^{2-}$  and  $\text{Fe}^{3+}$  estimates depends on the errors of cation estimation  
344 multiplied by their ionic charge.

Revision 1

345 The presence of A-cations in equations (4a,b) may be explained by their capability to help in  
346 achieving local electroneutrality around the O(3) site, where deprotonation occurs. Recent *in operando*  
347 studies combining SREF and FTIR (Fourier Transform Infrared Spectroscopy) showed that  
348 deprotonation preferentially occurs close to an occupied *A* site, so that it is faster in amphibole  
349 compositions with fully occupied A-sites (Susta et al. 2016; Della Ventura et al. 2017; Oberti et al.  
350 2018).

351

### 352 **TOTAL COEFFICIENT AND CALCULATION PROCEDURE**

353 In the previous section, we have stressed that the application of equation 2 is biased by the inevitable  
354 EMP errors of the 114 high-quality amphibole data (Fig. 1). In order to overcome this problem,  
355 obtaining an adjusted composition approaching a normalized one, we first calculated deviated  
356 compositions which are the concentrations (wt%) of the oxides and halogens (F, Cl) calculated from a  
357 normalized amphibole composition to have a *TEO* deviating from 100 wt% by a specific value, namely  
358 98.2 and 101.8 wt%; e.g., normalized  $\text{SiO}_2 \cdot 0.982$  (wt%), normalized  $\text{F} \cdot 1.018$  (wt%). The opposites of  
359 0.982 and 1.018 represent the corresponding total coefficients (*TC*) which, in general, can be calculated  
360 by dividing the sum of the oxides of a normalized composition by that of its original or deviated  
361 compositions. The *TC* values are 1 for normalized compositions, < 1 for overestimated compositions  
362 and > 1 for underestimated compositions.

363 Then we used equations 2 and 3 to calculate preliminary formulas for both normalized and deviated  
364 compositions. The values of  $\text{Fe}_2\text{O}_3$  and FeO concentrations,  $\text{O}^{\text{F,Cl}}$ , and  $\Delta\text{charge}$  can also be calculated  
365 from these preliminary unit-formulae (Appendix 1). Multivariate least-square analysis using all of these  
366 342 (114 normalized and 114·2 deviated) data provided the following equation to be used to calculate  
367 *TC*:



Revision 1

$$\begin{aligned} 368 \quad TC = & -7.9 * 10^{-4}SiO_2 + 6 * 10^{-4}TiO_2 - 6.6 * 10^{-4}Al_2O_3 + 8.75 * 10^{-5}Fe_2O_3 - 9.4 * 10^{-4}FeO - \\ 369 \quad & 8.5 * 10^{-4}MgO - 1.1 * 10^{-3}CaO - 1.48 * 10^{-3}Na_2O - 8.6 * 10^{-4}K_2O - 9.62 * 10^{-3}O^{F,Cl} + \\ 370 \quad & 6.41 * 10^{-3}H_2O - 9.57 * 10^{-3}TEO + 4.13 * 10^{-4}\Delta charge + 2.024 \quad (5) \end{aligned}$$

371 where SiO<sub>2</sub> to K<sub>2</sub>O are the original, normalized or the deviated oxides (wt%). The calculated regression  
372 parameters are R<sup>2</sup> = 0.992 and σ<sub>est</sub> = 0.001 (Fig. 3).

373 If the *TC* values are applied to the original EMP analyses (i.e., original SiO<sub>2</sub>·*TC*, original TiO<sub>2</sub>·*TC*,  
374 etc.), the resulting adjusted compositions closely approach the normalized concentrations (wt%). These  
375 adjusted compositions can then be used to obtain amphibole formulae using again equations (2) and  
376 (3). Using the 114 amphiboles in our high-quality dataset, this second stage of calculations produces a  
377 statistic error (σ<sub>est</sub>) of 0.055 apfu for ΣSi→K. The resulting formulae should be refined further using  
378 the series of stoichiometric constraints reported in Table 1 (see Appendix 1 for calculation).

379 When applying these constraints to the apfu calculated from the calibration dataset, only sporadic  
380 and very minor adjustments are observed (a few calculated formulae indicate ΣSi-K slightly higher  
381 than 16 apfu). In this dataset, the calculated *TEO* span from 99.6 to 100.5 wt%, and the final σ<sub>est</sub> values  
382 for <sup>A</sup>(Ca+Na+K) and Si contents are 0.042 and 0.017 apfu, respectively (Table 3). The amount of Fe<sup>3+</sup>  
383 (and Fe<sup>2+</sup>) can then be calculated by charge balance (eq. 4c).

384 Optionally, the <sup>W</sup>O<sup>2-</sup> and Fe<sup>3+</sup> contents can be independently estimated using a system of two linear  
385 equations, i.e., 4a and 4c. The total amount of Fe<sup>2+</sup> is finally calculated by the constraint Fe<sub>tot</sub> = Fe<sup>3+</sup> +  
386 Fe<sup>2+</sup> (Table 1, Appendix 1). The condition expressed in the constraint 4b should be respected and the  
387 priority in adjusting <sup>W</sup>O<sup>2-</sup> and Fe<sup>3+</sup> values should be given to charge balance (i.e., eq. 4c) considering  
388 that *Δcharge* can be as high as 0.1 due to error propagation in the solutions of this system.

389 Finally, the calculated amphibole formula (AMFORM) can be used to calculate the molecular mass  
390 (*M<sub>r</sub>*), hereafter *M<sub>r</sub>*<sup>AMFORM</sup> (see section Essential Definitions for *M<sub>r</sub>* calculation from a generic formula).

Revision 1

391  $M_r^{AMFORM}$  should closely approach the molecular mass calculated with equation 1 using the  $CR$  value  
392 obtained after the application of equation 1 to the adjusted compositions (hereafter  $M_r^{CR} = 10^3 \cdot CR$   
393 g/mol). In our database, the deviation among these molecular masses ( $\Delta MM\% = 200 \frac{M_r^{AMFORM} - M_r^{CR}}{M_r^{AMFORM} + M_r^{CR}}$ )  
394 ranges between -0.60 and 0.74% ( $\sigma_{est} = 0.18$ ; Table 3).

395 A flowchart and a step by step procedure to calculate amphibole unit-formulae are reported in  
396 Appendix 1. The whole procedure is included in a user-friendly Excel spreadsheet (provided as  
397 supplementary material) called AMFORM.xlsx. By default, this spreadsheet gives the  $^{W}O^{2-}$  and  $Fe^{3+}$   
398 values calculated according to equations 3 and 4c, but it also gives the results of the optional method  
399 (eqs. 4a-c). We strongly recommend the use of this spreadsheet to avoid errors due to typing or  
400 unavoidable approximations of the coefficients reported in this article.

401 AMFORM.xlsx also provides warnings for bad analyses and deviations from the correct  
402 stoichiometry such as recalculated initial  $TEO < 98.2$  and  $> 101.8$  wt%, sum of C and B cations  $< 5$  and  
403 2 apfu, respectively (i.e., negative  $\Delta C$  and Ca in A-group) and  $\Delta MM\% < -0.60$  and  $> 0.74\%$ , which are  
404 not included in Appendix 1.

405

## 406 TESTING THE AMFORM APPROACH

407 To allow for an independent validation of the AMFORM approach, a test was made using an additional  
408 51 amphibole compositions belonging to the Ca, Na-Ca, Na and oxo groups, taken from the literature  
409 (King et al. 2000; Tiepolo et al. 2001; Oberti et al. 2000, 2003, 2010, 2015, 2016, 2017; Uvarova et al.  
410 2007; Satoh et al. 2004; Della Ventura et al. 2014; Gentili et al. 2015; Gatta et al. 2017) or still  
411 unpublished (CNR-IGG Pavia), which have been analyzed with EMP $\pm$ SREF $\pm$ SIMS and other  
412 techniques for  $Fe^{3+}/Fe_{tot}$  measurements ( $KMnO_4$  titration, SXRF, XANES, Mössbauer spectroscopy). It  
413 is worth noting that the analyses of these amphiboles generally have higher uncertainties (e.g.,  $TEO$  of

Revision 1

414 97-102 wt%;  $dC$  from -0.07 to 0.01 apfu;  $\Delta charge$  from -0.09 to 0.07) than the 114 analyses selected  
415 for the calibration of the AMFORM procedure (see the AMFORM spreadsheet for these lower-quality  
416 data). This second test dataset also includes 10 amphibole composition-formula pairs recently  
417 published by Dyar et al. (2016) respecting the quality criteria of the calibration data (AMFORM.xlsx).

418 Table 3 and Figure 4 compare the capability of AMFORM to estimate the amphibole formula  
419 parameters for both the calibration and the test data. The generally higher  $\sigma_{est}$  values of the lower-  
420 quality test data confirm the validity of our approach while the higher  $\Delta MM\%$  values indicate that this  
421 parameter is useful for detecting large analytical uncertainties (Table 3). The reliability of AMFORM is  
422 further confirmed by the homogeneous distribution around the 1:1 line observed for both calibration  
423 and test data and by the absence of outliers (Fig. 4). The few Li-free Na amphibole used to test  
424 AMFORM suggest that the method is reliable also in the case of Na amphiboles (e.g., Fig. 4c), for  
425 which the calibration was based solely on end-member compositions (Table 2; Fig. 1b). A test  
426 performed using 28 Fe-Mg-Mn  $C2/m$  species (cummingtonite-grunerite; Hirschmann et al. 1994) also  
427 suggest that AMFORM.xlsx can be used for these amphiboles with reasonably low uncertainties ( $\sigma_{est} \leq$   
428 0.040 apfu for the main cations). However, this test is not reliable because Hirschmann et al. (1994)  
429 calculated the formula under the constraint that  $\sum Si \rightarrow K = 15$ .

430

### 431 **A comparison between the AMFORM and the Locock (2014) spreadsheets**

432 As a final step, we tested the capability of the most used methods to calculate the amphibole unit-  
433 formula (i.e., Tindle and Webb 1994; Dale et al. 2005; Locock 2014) using our calibration and test  
434 datasets (electronic supplement 1). For most compositions, the PROBE-AMPH spreadsheet (Tindle and  
435 Webb 1994) and the model of Dale et al. (2005) (which is an improvement of that of Holland and  
436 Blundy 1994) give errors which are about twice those of Locock (2014) and will be not discussed  
437 further.

Revision 1

438 When calculating the amphibole unit-formula, the most difficult parameters to quantify are the  $^C\text{Al}$  and  
439  $\text{Fe}^{3+}$  contents and the amount of cations in A, i.e.,  $^A(\text{Ca} + \text{Na} + \text{K})$  (e.g., Leake et al. 1997; Al'meev et  
440 al. 2002; Ridolfi et al. 2010). Figure 5, compares the AMFORM results obtained for these parameters  
441 with those calculated by the spreadsheet published by Locock (2014), which is based on the procedures  
442 suggested in the IMA 2012 classification scheme (Hawthorne et al. 2012). When the  $\text{Fe}^{3+}/\text{Fe}_{\text{tot}}$  ratio,  
443 and/or the  $\text{H}_2\text{O}$  and Li contents are unknown (i.e., when only EMP analyses are available), the Locock  
444 (2014) spreadsheet provides two automatic procedures, depending on the presence or absence of  $^W\text{O}^{2-}$ .  
445 The  $\text{Fe}^{3+}$  contents resulting from AMFORM are those of the default  $^W\text{O}^{2-}$  method (eq. 3 and 4c). As a  
446 matter of fact, considering the unit-formulae of the high-quality amphibole compositions as reference  
447 data (i.e., those cation contents that for their high-quality better approach the effective unit formulae),  
448 the errors of the AMFORM procedure are, on average, 2 to 4 times lower than those obtained with the  
449 spreadsheet proposed by Locock (2014) (Fig. 5).

450 Locock (2014) tends to underestimate  $^C\text{Al}$  and  $^A(\text{Ca} + \text{Na} + \text{K})$  in amphiboles with total cation  
451 contents close to 16 apfu, and to slightly overestimate the same parameters when the  $\sum\text{Si-K}$  is close to  
452 15 apfu. As far as the  $\text{Fe}^{3+}$  content is concerned, Locock (2014) methods with and without  $^W\text{O}^{2-}$   
453 estimates, behaves similarly to the 13- and 15-cations methods by IMA-1997 (Leake et al. 1997) as  
454 they generally produce large overestimations and large underestimations, respectively (Fig. 5).

455 For an independent validation of the AMFORM approach and Locock (2014)'s methods, we  
456 tested a subset of 19 published compositions of poorly-oxidized amphiboles (yellow squares in Fig. 5c;  
457 AMFORM spreadsheet). These data were not included in our high-quality calibration dataset because  
458 they were recently published, have not been examined by SREF and/or or because they have high  
459  $\Delta\text{charge}$  values (up to  $\pm 0.13$ ). However, the  $\text{Fe}^{3+}$  content (and  $\text{Fe}^{3+}/\text{Fe}_{\text{tot}}$ ) of these amphiboles should  
460 be valuable as it was estimated by SREF and Mössbauer spectroscopic analyses (Dyar et al. 2016),  
461 Synchrotron X-ray Fluorescence (SXRF; King et al. 2000),  $\text{KMnO}_4$  titration (Satoh et al. 2004) or X-ray

Revision 1

462 Absorption Near Edge Structure (XANES) spectroscopy (Bonadiman et al. 2014). In the AMFORM  
463 (default method) and Locock (2014) diagrams (Figs. 5c,f,i), these 19 amphiboles with  ${}^W\text{O}^{2-} < 2\text{Ti}$  have  
464 the same behavior as the poorly-oxidized calibration amphiboles. When the reference  $\text{Fe}^{3+}$  values of  
465 these amphiboles are compared to those obtained by AMFORM, they approach the 1:1 line and have  
466 deviations (from -0.14 to +0.27 apfu) well within the maximum-minimum  $\text{Fe}^{3+}$  error range of the  
467 AMFORM default procedure (Fig. 5c).

468

#### 469 **An evaluation of the two methods used by AMFORM to calculate ${}^W\text{O}^{2-}$ and $\text{Fe}^{3+}$**

470 Figure 6 reports plots and statistics obtained by using the AMFORM default (eq. 3, 4c) and the optional  
471 (eq. 4a-c) methods to calculate the  ${}^W\text{O}^{2-}$  and  $\text{Fe}^{3+}$  contents for 137 amphibole compositions (114 high-  
472 quality compositions used for calibration plus 23 among lower-quality compositions and recently  
473 published data, both poorly and highly oxidized) where  $\text{Fe}^{3+}/\text{Fe}_{\text{tot}}$  values were measured as discussed in  
474 the previous paragraph and in Figure 5c.

475 The default method in AMFORM is particularly useful to estimate the amount of  ${}^W\text{O}^{2-}$  and  $\text{Fe}^{3+}$   
476 in poorly-oxidized amphiboles, those in equilibrium with the melt and/or other minerals (e.g., at 800–  
477 1,130 C, 130–2,200 MPa and in between NNO-2.1 and NNO+3.6; Ridolfi and Renzulli 2012). Indeed,  
478 these amphiboles fall very close to (and are distributed homogeneously around) the 1:1 line in Figures  
479 6a,b; their  ${}^W\text{O}^{2-}$  and  $\text{Fe}^{3+}$  contents can be estimated with a reasonably low uncertainty ( $\pm 0.1$  apfu; Table  
480 3; Figs. 2a and 4c). In contrast, in the case of highly-oxidized amphiboles, i.e., those which underwent  
481 hydrothermal and post-crystallization oxidation, the default method may provide significant  
482 underestimation (up to 1.1 apfu,  $\sigma_{\text{est}} = 0.45$  apfu; Fig. 6a,b), and therefore cannot be used to study  
483 metasomatic and oxidation processes during magma ascent (Dyar et al. 1993; King et al. 1999; Popp et  
484 al. 2006; Oberti et al. 2007a). Hence, we suggest to use the optional method for these amphiboles,  
485 because it provides a roughly homogeneous distribution around the 1:1 line in the plots in Figures 6d,e.

Revision 1

486 The large observed uncertainties when estimating  $^{\text{W}}\text{O}^{2-}$  and  $\text{Fe}^{3+}$  values by this method (up to 1.1 apfu,  
487  $\sigma_{\text{est}} = 0.3$  apfu; Table 3) occur because of the substantial propagation of errors from the system of two  
488 linear equations (eq. 4a and 4c) and two variables ( $^{\text{W}}\text{O}^{2-}$  and  $\text{Fe}^{3+}$ ). Indeed, Table 3 also reports the  
489 estimated  $\text{Fe}^{3+}$  error due to uncertainty propagation (according to the probability theory), for both  
490 default and optional calculations. When calculated using the uncertainties of the calibration higher-  
491 quality dataset, the propagation of  $\text{Fe}^{3+}$  errors in the optional method are about twice of those in the  
492 default calculation and almost double when the quality of the data is lowered (i.e. when using the errors  
493 of the lower-quality test dataset). However, Figures 6c,f show that the error in  $\text{Fe}^{3+}/\text{Fe}_{\text{tot}}$  determination  
494 tends to decrease regularly with increasing total iron content ( $\text{Fe}_{\text{tot}}$ ) for both the default (only  
495 considering the poorly-oxidized amphiboles) and the optional method. In other words, the tested  
496 amphiboles show a homogeneous and decreasing distribution around the zero-error line (Figs 6c,f). It is  
497 worth noting that the most used methods for unit-formula calculation (Tindle and Webb 1994; Dale et  
498 al. 2005; Locock 2014) result in much more scattered distributions of the  $\text{Fe}^{3+}/\text{Fe}_{\text{tot}}$  errors and higher  
499  $\sigma_{\text{est}}$  values (electronic supplement 1). For Fe-Mg-Mn amphiboles such as cummingtonite and grunerite,  
500 we recommend the use of the optional method. We have tested AMFORM against the data of  
501 Hirschmann et al. (1994) indicating an  $\text{Fe}^{3+}/\text{Fe}_{\text{tot}} \leq 1\%$  for heat-treated Fe-Mg-Mn amphiboles, as  
502 measured by Mössbauer spectroscopy (see above). For these amphiboles, the optional method shows  
503  $\text{Fe}^{3+}/\text{Fe}_{\text{tot}} < 5\%$  ( $\leq 1\%$  for most of them, 71%) whereas the default method indicates higher  $\text{Fe}^{3+}/\text{Fe}_{\text{tot}}$   
504 values (up to 17%).

505

506

## IMPLICATIONS

507 Figure 4 and Table 3 demonstrate the capability of the AMFORM approach to quantify, based solely  
508 on EMP data, the most critical parameters in the unit formula of amphiboles with a satisfactory

Revision 1

509 reliability. It is worth noting that the proposed approach has been calibrated and is consistent with  
510 crystal-chemical formulae obtained by combining high-quality structure refinement and analytical data.

511 The AMFORM procedure has been calibrated and validated for some petrologically-relevant  
512 *C2/m* amphibole compositions (oxo, Ca, Na-Ca, Na, Fe-Mg-Mn amphiboles), considering only Li- and  
513 Mn<sup>3+</sup>-free end-member compositions. The presence of significant Li and Cl contents would strongly  
514 affect the results because their lower cation mass and higher anion mass, respectively, would largely  
515 affect the behavior of the *CR-cmpg* relationship. Indeed, AMFORM should be applied only to  
516 amphiboles with Cl < 0.2 apfu (<1 wt%). In addition, AMFORM only accounts for Mn<sup>2+</sup> and hence  
517 cannot be used to constrain the formula of Mn<sup>3+</sup>-rich amphiboles (e.g., dellaventuraite, ungarrettiite;  
518 Hawthorne et al. 1995; Hawthorne et al. 2012).

519 However, AMFORM.xlsx automatically provides warnings anytime the composition proposed  
520 deviates too much from the calibration dataset and the calculated *TEO* values (both initial and adjusted)  
521 deviate too much from those shown by the calibration amphiboles.

522 The default AMFORM procedure to estimate <sup>W</sup>O<sup>2-</sup> and Fe<sup>3+</sup> contents is particularly  
523 recommended to study the stability of amphibole and develop (or refine) thermobarometric equations  
524 aiming at constraining the magma pre-eruptive conditions and storage from the amphibole composition  
525 of volcanic rocks (e.g., Ridolfi et al. 2010; Ridolfi and Renzulli 2012; Erdmann et al. 2014; Putirka  
526 2016; Ridolfi et al. 2016). For this purpose, the difficulty of estimating the Fe<sup>3+</sup> content related to  
527 hydrothermal or post-magmatic oxidizing processes may even be considered as an advantage (see  
528 above). In any case, this Fe<sup>3+</sup> component can be roughly estimated using the optional <sup>W</sup>O<sup>2-</sup> and Fe<sup>3+</sup>  
529 results in AMFORM.xlsx.

530 The mass-based method proposed in this work may also open a new perspective in the  
531 calculation of the unit-formula of other minerals. It may be particularly useful for OH-bearing phases  
532 characterized by structural vacancies, where the total number of cation is not known (e.g., micas).

Revision 1

533 While equation 1 is valid for any type of chemical compound and mineral, equation 2 must be adapted  
534 to other phases with different proportions of anion and cation sites in order to allow a reliable estimate  
535 of  $CR$ , and thus, of the total cation apfu contents.

536

### 537 **Acknowledgments**

538 This work was supported by a fellowship of the Alexander Von Humboldt Foundation and a research  
539 grant (“assegno di ricerca”) co-funded by University of Perugia and University of Urbino through the  
540 Consolidator Grant ERC-2013- CoG Proposal No. 612776 CHRONOS (P.I. Diego Perugini), both  
541 awarded to the first author. AZ and RO acknowledge support by the Italian PRIN 2015 grant code  
542 20158 A9CBM. We are grateful to R.R. Al’meev and O. Namur (Leibniz Universität Hannover) for  
543 their critical readings of the manuscript.

544 Careful and helpful reviews of the manuscript done by two anonymous referees greatly improved the  
545 quality of the manuscript. We thank them very much for all their suggestions.

546

### 547 **References**

548 Adam J., Oberti R., Cámara F., and Green T.H. (2007) An electron microprobe, LAM-ICP-MS and  
549 single-crystal X-ray structure refinement study of the effect of pressure, melt-H<sub>2</sub>O concentration  
550 and fO<sub>2</sub> on experimentally produced basaltic amphiboles. *European Journal of Mineralogy*, 19,  
551 641–655.

552 Al’meev R.R., Ariskin A.A., Ozerov A.Yu., and Kononkova N.N. (2002) Problems of the  
553 Stoichiometry and Thermobarometry of Magmatic Amphiboles: An Example of Hornblende



Revision 1

- 554 from the Andesites of Nezymyannyi Volcano, Eastern Kamchatka. *Geochemistry International*,  
555 40, 723-738.
- 556 Bonadiman C., Nazzareni S., Coltorti M., Comodi P., Giuli G., and Faccini B. (2014) Crystal chemistry  
557 of amphiboles: implications for oxygen fugacity and water activity in lithospheric mantle  
558 beneath Victoria Land, Antarctica. *Contributions to Mineralogy and Petrology*, 167, 984.
- 559 Bottazzi P., Tiepolo M., Vannucci R., Zanetti A., Brumm R., Foley S.F., and Oberti R. (1999) Distinct  
560 site preferences for heavy and light REE in amphibole and the prediction of  $^{Amph/L}D_{REE}$ .  
561 *Contributions to Mineralogy and Petrology*, 137, 36-45.
- 562 Cipriani C. (2007) Amphiboles: Historical Perspective. *Reviews in Mineralogy and Geochemistry*, 67,  
563 517-546.
- 564 Coogan L.A., Wilson R.N., Gillis K.M., and MacLeod C.J. (2001) Near-solidus evolution of oceanic  
565 gabbros: insights from amphibole geochemistry. *Geochimica et Cosmochimica Acta*, 65, 4339–  
566 4357.
- 567 Dale J., Powel R., White R.W., Elmer F.L., and Holland T.J.B. (2005) A thermodynamic model for  
568 Ca–Na clin amphiboles in  $Na_2O$ – $CaO$ – $FeO$ – $MgO$ – $Al_2O_3$ – $SiO_2$ – $H_2O$ – $O$  for petrological  
569 calculations. *Journal of Metamorphic Geology*, 23, 771–791.
- 570 Della Ventura G., Bellatreccia F., Cámara F., and Oberti R. (2014) Crystal-chemistry and short-range  
571 order of fluoro-edenite and fluoro-pargasite: a combined X-ray diffraction and FTIR  
572 spectroscopic approach. *Mineralogical Magazine*, 78, 293-310.

Revision 1

- 573 Della Ventura G., Susta U., Bellatreccia F., Marcelli A., Redhammer G.J., and Oberti R. (2017)  
574 Deprotonation of Fe-dominant amphiboles: Single-crystal HT-FTIR spectroscopic studies of  
575 synthetic potassic-ferro-richterite. *American Mineralogist*, 102, 117-125.
- 576 Dyar M.D., Mackwell S.J., McGuire A.V., Cross L.R., and Robertson J.D. (1993) Crystal chemistry of  
577 Fe<sup>3+</sup> and H<sup>+</sup> in mantle kaersutite: Implications for mantle metasomatism. *American Mineralogist*,  
578 78, 968-979.
- 579 Dyar M.D., Breves E.A., Gunter M.E., Lanzirotti A., Tucker J.M., Carey C.J., Peel S.E., Brown E.B.,  
580 Oberti R., Lerotic M., and Delaney J.S. (2016) Use of multivariate analysis for synchrotron  
581 micro-XANES analysis of iron valence state in amphiboles. *American Mineralogist*, 101, 1171–  
582 1189.
- 583 Erdmann S., Martel C., Pichavant M., and Kushnir A. (2014) Amphibole as an archivist of magmatic  
584 crystallization conditions: problems, potential, and implications for inferring magma storage  
585 prior to the paroxysmal 2010 eruption of Mount Merapi, Indonesia. *Contributions to Mineralogy  
586 and Petrology*, 167, 1016.
- 587 Esawi E.K. (2004) AMPH-CLASS: An Excel spreadsheet for the classification and nomenclature of  
588 amphiboles based on the 1997 recommendations of the International Mineralogical Association.  
589 *Computers & Geosciences* 30, 753–760.
- 590 Foley S., Tiepolo M., and Vannucci R. (2002) Growth of early continental crust controlled by melting  
591 of amphibolite in subduction zones. *Nature*, 417, 837-840.
- 592 Forbes W.C., and Starmer R.J. (1974) Kaersutite is a possible source of alkali olivine basalts. *Nature*,  
593 250, 209-210.

Revision 1

- 594 Gatta G.D., McIntyre G.J., Oberti R., and Hawthorne F.C. (2017) Order of  $^{[6]}\text{Ti}^{4+}$  in a Ti-rich calcium  
595 amphibole from Kaersut, Greenland: a combined X-ray and neutron diffraction study. *Physics*  
596 *and Chemistry of Minerals*, 44, 83-94.
- 597 Gentili S., Bonadiman C., Biagioni C., Comodi P., Coltorti M., Zucchini A., and Ottolini L. (2015)  
598 Oxo-amphiboles in mantle xenoliths: evidence for H<sub>2</sub>O-rich melt interacting with the  
599 lithospheric mantle of Harrow Peaks (Northern Victoria Land, Antarctica). *Minerogy and*  
600 *Petrology*, 109, 741-759.
- 601 Gunter M.E., Belluso E., and Mottana A. (2007) Amphiboles: Environmental and health concerns.  
602 *Reviews in Mineralogy and Geochemistry*, 67, 453-516.
- 603 Hammarstrom J.M., and Zen E. (1986) Aluminum in hornblende: an empirical igneous geobarometer.  
604 *American Mineralogist*, 71, 1297-1313.
- 605 Häuy R.J. (1822) *Traité de Minéralogie*. II ed. Bachelier-Huzard, Paris, pp. 597.
- 606 Hawthorne F.C., Ungaretti L., Oberti R., Bottazzi P., and Czamanske G.K. (1993) Li: An important  
607 component in igneous alkali amphiboles. *American Mineralogist*, 78, 733-745.
- 608 Hawthorne F.C. (1983) The crystal chemistry of the amphiboles. *The Canadian Mineralogist*, 21, 173-  
609 480 .
- 610 Hawthorne F.C., Oberti R., Cannillo E., Sardone N., Zanetti A., Grice J.D., and Ashley P.M. (1995). A  
611 new anhydrous amphibole from the Hoskins mine, Grenfell, New South Wales, Australia:  
612 Description and crystal structure of ungarrettiite,  $\text{NaNa}_2(\text{Mn}_2^{2+}\text{Mn}_3^{3+})\text{Si}_8\text{O}_{22}\text{O}_2$ . *American*  
613 *Mineralogist*, 80, 165-172.

Revision 1

- 614 Hawthorne F.C., Oberti R., Della Ventura G., and Mottana A. (2007) Amphiboles: Crystal Chemistry,  
615 Occurrence, and Health Issues. *Reviews in Mineralogy and Geochemistry*, 67, 545 pp
- 616 Hawthorne F.C., Oberti R., Harlow G.E., Maresch W.V., Martin R.F., Schumacher J.C., and Welch  
617 M.D. (2012) IMA report Nomenclature of the amphibole supergroup. *American Mineralogist*,  
618 97, 2031-2048.
- 619 Hawthorne F.C., Oberti R., Cannillo E., Ottolini L., Roelofsen J.N., and Martin R.F. (2001) Li-bearing  
620 arfvedsonitic amphiboles from the Strange Lake peralkaline granite, Quebec. *The Canadian*  
621 *Mineralogist*, 39, 1161-1170.
- 622 Hirschmann M., Evans B.W., and Yang H. (1994) Composition and temperature dependence of Fe-Mg  
623 ordering in cummingtonite-grunerite as determined by X-ray diffraction. *American Mineralogist*  
624 79, 862-877.
- 625 Holland T.J.B., and Blundy J.D. (1994) Non-ideal interactions in calcic amphiboles and their bearing  
626 on amphibole-plagioclase thermometry. *Contributions to Mineralogy and Petrology*, 116, 433-  
627 447.
- 628 Jackson C.R.M., Parman S.W., Kelley S.P., and Cooper R.F. (2013) Noble gas transport into the  
629 mantle facilitated by high solubility in amphibole. *Nature Geoscience*, 6, 562-565.
- 630 Jacobson C.E., and Sorensen S.S. (1986) Amphibole compositions and metamorphic history of the  
631 Rand Schist and the greenschist unit of the Catalina Schist, Southern California. *Contributions to*  
632 *Mineralogy and Petrology*, 92, 308-315.
- 633 King P.L., Hervig R.L., Holloway J.R., Vennemann T.W., and Righter K. (1999) Oxy-substitution and  
634 dehydrogenation in mantle-derived amphibole megacrysts. *Geochimica et Cosmochimica Acta*,  
635 63, 3635-3651.

Revision 1

- 636 King P.L., Hervig R.L., Holloway J.R., Delaney J.S., and Dyar M.D. (2000) Partitioning of  $\text{Fe}^{3+}/\text{Fe}_{\text{total}}$   
637 between amphibole and basanitic melt as a function of oxygen fugacity. *Earth and Planetary*  
638 *Science Letters*, 178, 97-112.
- 639 Laird J.O., and Albee A.L. (1981) High-pressure metamorphism in mafic schist from Northern  
640 Vermont. *American Journal of Science*, 281, 97-126.
- 641 Léger A., Rebert C., and Webster J. (1996) Cl-rich biotite and amphibole from Black Rock Forest,  
642 Cornwall, New York. *American Mineralogist*, 81, 495–504.
- 643 Leake B.E. (1978) Nomenclature of amphiboles. *The Canadian Mineralogist*, 16, 501-520.
- 644 Leake B.E., Woolley A.R., Arps C.E.S., Birch W.D., Gilbert M.C., Grice J.D., Hawthorne F.C., Kato  
645 A., Kisch H.J., Krivovichev V.G., Linthout K., Laird J., Mandarino J., Maresch W.V., Nickel  
646 E.H., Schumaker J.C., Smith D.C., Stephenson N.C.N., Ungaretti L., Whittaker E.J.W., and  
647 Youzhi G. (1997) Nomenclature of amphiboles: report of the subcommittee on amphiboles of  
648 the International Mineralogical Association Commission on New Minerals and Mineral Names.  
649 *Mineralogical Magazine*, 61, 295-321.
- 650 Locock A.J. (2014) An Excel spreadsheet to classify chemical analyses of amphiboles following the  
651 IMA2012 recommendations. *Computer and Geosciences*, 62, 1–11.
- 652 McCanta M.C., Treiman A.H., Dyar M.D., Alexander C.M.O.'D., Rumble III D., and Essene E.J.  
653 (2008) The LaPaz Icefield 04840 meteorite: Mineralogy, metamorphism, and origin of an  
654 amphibole-and biotite-bearing R chondrite. *Geochimica et Cosmochimica Acta*, 72, 5757-5780.
- 655 Oberti R., Ungaretti L., Cannillo E., Hawthorne F.C., and Memmi I. (1995) Temperature-dependent Al  
656 order-disorder in the tetrahedral double chain of C2/m amphiboles. *European Journal of*  
657 *Mineralogy*, 7, 1049-1063.

Revision 1

- 658 Oberti R., Vannucci R., Zanetti A., Tiepolo M., and Brumm R.C. (2000) A crystal chemical re-  
659 evaluation of amphibole/melt and amphibole/clinopyroxene  $D_{Ti}$  values in petrogenetic studies.  
660 American Mineralogist, 85, 407-419.
- 661 Oberti R., Boiocchi M., and Smith D.C. (2003) Fluoronyböite from Jianchang (Su-Lu, China) and  
662 nyböite from Nybö (Nordfjord, Norway): a petrological and crystal-chemical comparison of  
663 these two high-pressure amphiboles. Mineralogical Magazine, 67, 769–782.
- 664 Oberti R., Hawthorne F.C., Cannillo E., and Cámara F. (2007a) Long-range order in amphiboles.  
665 Reviews in Mineralogy and Geochemistry, 67, 125-171.
- 666 Oberti R., Boiocchi M., Smith D.C., and Medenbach O. (2007b) Aluminotaramite, alumino-  
667 magnesiotalamite, and fluoro-alumino-magnesiotalamite: Mineral data and crystal chemistry.  
668 American Mineralogist, 92, 1428-1435.
- 669 Oberti R., Boiocchi M., Hawthorne F.C., and Robinson P. (2010) Crystal structure and crystal  
670 chemistry of fluoro-potassic-magnesian-arfvedsonite from Monte Metocha, Xixano region,  
671 Mozambique, and discussion of the holotype from Quebec, Canada. Mineralogical Magazine,  
672 74, 951-960.
- 673 Oberti R., Boiocchi M., Hawthorne F.C., Ball N.A., and Harlow G.E. (2015) Katophorite from the Jade  
674 Mine Tract, Myanmar: mineral description of a rare (grandfathered) endmember of the  
675 amphibole supergroup. Mineralogical Magazine, 79, 355–363.
- 676 Oberti R., Boiocchi M., Hawthorne F.C., Ball N.A., Cámara F., Pagano R., and Pagano A. (2016)  
677 Ferro-ferri-hornblende from the Traversella Mine (Ivrea, Italy): occurrence, mineral description  
678 and crystal-chemistry. Mineralogical Magazine, 80, 1233-1242.

Revision 1

- 679 Oberti R., Boiocchi M., Hawthorne F.C., Ball N.A., and Blass G. (2017) Ferri-obertiite from the  
680 Rothenberg quarry, Eifel volcanic complex, Germany: mineral data and crystal chemistry of a  
681 new amphibole end-member. *Mineralogical Magazine*, press. DOI: 10.1127/ejm/2018/0030-  
682 2712.
- 683 Oberti R., Boiocchi M., Zema M., Hawthorne F.C., Redhammer G., Susta U., and Della Ventura G.  
684 (2018) The HT behaviour of riebeckite: Expansivity, deprotonation, selective Fe oxidation and a  
685 novel cation disordering scheme for amphiboles. *European Journal of Mineralogy*, press. DOI:  
686 10.1127/ejm/2018/0030-2712.
- 687 Ottolini L., Bottazzi P., Zanetti A., and Vannucci R. (1995) Determination of hydrogen in silicates by  
688 Second Ion Mass Spectrometry. *The Analyst*, 120, 1309-1314.
- 689 Namur O., Charlier B., Toplis M.J., and Auwera J.V. (2012) Prediction of plagioclase-melt equilibria  
690 in anhydrous silicate melts at 1 atm. *Contributions to Mineralogy and Petrology*, 163, 133-150.
- 691 Perinelli C., Andreozzi G.B., Conte A.M., Oberti R., and Armienti P. (2012) Redox state of  
692 subcontinental lithospheric mantle and relationships with metasomatism: insights from spinel  
693 peridotites from northern Victoria Land (Antarctica). *Contributions to Mineralogy and  
694 Petrology*, 164, 1053-1067.
- 695 Popp R.K., Hibbert H.A., and Lamb W.M. (2006) Oxy-amphibole equilibria in Ti-bearing calcic  
696 amphiboles: Experimental investigation and petrologic implications for mantle-derived  
697 amphiboles. *American Mineralogist*, 91, 54-66.
- 698 Putirka K. (2016) Amphibole thermometers and barometers for igneous systems and some implications  
699 for eruption mechanisms of felsic magmas at arc volcanoes. *American Mineralogist*, 101, 841-  
700 858.

Revision 1

- 701 Ridolfi F., Renzulli A., and Puerini M. (2010) Stability and chemical equilibrium of amphibole in calc-  
702 alkaline magmas: an overview, new thermobarometric formulations and application to  
703 subduction-related volcanoes. *Contributions to Mineralogy and Petrology*, 160, 45-66.
- 704 Ridolfi F., and Renzulli A. (2012) Calcic amphiboles in calc-alkaline and alkaline magmas:  
705 thermobarometric and chemometric empirical equations valid up to 1,130°C and 2.2 GPa.  
706 *Contributions to Mineralogy and Petrology*, 163, 877-895.
- 707 Ridolfi F., Renzulli A., and Acosta-Vigil A. (2014) On the stability of magmatic cordierite and new  
708 thermobarometric equations for cordierite-saturated liquids. *Contributions to Mineralogy and*  
709 *Petrology*, 167, 996.
- 710 Ridolfi F., Braga R., Cesare B., Renzulli A., Perugini D., and Del Moro S. (2016) Unravelling the  
711 complex interaction between mantle and crustal magmas encoded in the lavas of San Vincenzo  
712 (Tuscany, Italy). Part I: Petrography and Thermobarometry. *Lithos*, 244, 218-232.
- 713 Robinson G.W., Grief J.D., Gault R.A., and Lalonde A.E. (1997) Potassic pargasite, a new member of  
714 the amphibole group from Pargas, Turku-Pori, Finland. *The Canadian Mineralogist*, 35, 1535-  
715 1540.
- 716 Rock N.M.S., and Leake B.E. (1984) The International Mineralogical Association amphibole  
717 nomenclature scheme: computerization and its consequences. *Mineralogical Magazine*, 48, 211-  
718 227.
- 719 Satoh H., Ymaguchi Y., and Makino K. (2004) Ti-substitution mechanism in plutonic oxy-kaersutite  
720 from the Larvik alkaline complex, Oslo rift, Norway. *Mineralogical Magazine*, 68, 687-697.



Revision 1

- 721 Smith P.P.K. (1977) An Electron Microscopic Study of Amphibole Lamellae in Augite. Contributions  
722 to Mineralogy and Petrology, 59, 317-322.
- 723 Smith D.J. (2014) Clinopyroxene precursors to amphibole sponge in arc crust. Nature  
724 Communications, 5, 4329.
- 725 Spear F.S., and Kimball K.L. (1984). RECAMP—A FORTRAN IV program for estimating Fe<sup>3+</sup>  
726 contents in amphiboles. Computer and Geosciences, 10, 317-325.
- 727 Susta U. (2016) Dehydration and deprotonation processes in minerals: development of new  
728 spectroscopic techniques. Unpublished PhD Thesis, University of Roma Tre.
- 729 Stout J.H. (1972) Phase Petrology and Mineral Chemistry of Coexisting Amphiboles from Telemark,  
730 Norway. Journal of Petrology, 13, 99-145.
- 731 Tiepolo M., Vannucci R., Oberti R., Foley S., Bottazzi P., and Zanetti A. (2000) Nb and Ta  
732 incorporation and fractionation in titanian pargasite and kaersutite: crystal-chemical constraints  
733 and implications for natural systems. Earth and Planetary Science Letters, 176, 185-201.
- 734 Tiepolo M., Bottazzi P., Foley S.F., Oberti R., Vannucci R., and Zanetti A. (2001) Fractionation of Nb  
735 and Ta from Zr and Hf at Mantle Depths: the Role of Titanian Pargasite and Kaersutite. Journal  
736 of Petrology, 42, 221-232.
- 737 Tiepolo M., Zanetti A., Oberti R., Brumm R., Foley S., and Vannucci R. (2003) Trace-element  
738 partitioning between synthetic potassic-richterites and silicate melts, and contrasts with the  
739 partitioning behaviour of pargasites and kaersutites. European Journal of Mineralogy, 15, 329-  
740 340.
- 741 Tindle A.G., and Webb P.C. (1994) PROBE-AMPH—a spreadsheet program to classify microprobe-  
742 derived amphibole analyses. Computer and Geosciences, 20, 1201-1228.

Revision 1

- 743 Ungaretti L. (1980) Recent developments in X-ray single crystal diffractometry applied to the crystal-  
744 chemical study of amphiboles. *Godisnjak Jugoslavenskog Centra za Kristalografiju*, 15, 29-65.
- 745 Ungaretti L., Smith D.C., and Rossi G. (1981) Crystal-chemistry by X-ray structure refinement and  
746 electron microprobe analysis of a series of sodic-calcic to alkali amphiboles from the NybO  
747 eclogite pod, Norway. *Bulletin de Minéralogie*, 104, 400-412.
- 748 Uvarova Y., Sokolova E., Hawthorne F.C., McCammon C.A., Kazansky V.I., and Lobanov K.V.  
749 (2007) Amphiboles from the Kola Superdeep Borehole: Fe<sup>3+</sup> contents from crystal-chemical  
750 analysis and Mössbauer spectroscopy. *Mineralogical Magazine*, 71, 651-669.
- 751 Vannucci R., Piccardo G.B., Rivalenti G., Zanetti A., Rampone E., Ottolini L., Oberti R., Mazzucchelli  
752 M., and Bottazzi P. (1995) Origin of LREE-depleted amphiboles in the subcontinental mantle.  
753 *Geochimica et Cosmochimica Acta*, 59, 1763-1771.
- 754 Zhang J., Humphreys M.C.S., Cooper G.F., Davidson J.P., and Macpherson C.G. (2017) Magma mush  
755 chemistry at subduction zones, revealed by new melt major element inversion from calcic  
756 amphiboles. *American Mineralogist*, 102, 1353-1367.

Revision 1

757

758 **Table captions**

759 Table 1.

760 Summary of the preferred site-assignments and stoichiometric constraints for Li- and Mn<sup>3+</sup>-free *C2/m*  
761 amphiboles, according to Hawthorne et al. (2012).

762 Table 2.

763 Formula and normalized composition (wt%) of the selected Li- and Mn-free monoclinic amphibole  
764 end-members and the oxo counterparts for the Ca amphiboles considered in this work. As the  
765 composition is normalized, all total elements and oxides close to ideality (100 wt%). The end-embers  
766 are ordered by increasing *Mr*. Values of *cmpg* are also reported for comparison.

767 Table 3.

768 Statistic errors ( $\sigma_{\text{est}}$ ) of the AMFORM procedure calculated using the calibration and test data. The  
769 errors of uncertainty propagation in the calculation of the parameters are also reported. See  
770 AMFORM.xlsx for references and data.

771

772 **Figure captions**

773 Figure 1.

774 Plots of *CR* vs. (a) *Mr*, molecular mass, and (b) *cmpg*, cation mass per gram. The equations (and  
775 their statistic values) obtained using normalized and end-member (Table 2) compositions are also  
776 reported. The end-member sample with the lowest *Mr* is cummingtonite,  $\square\text{Mg}_2\text{Mg}_5\text{Si}_8\text{O}_{22}(\text{OH})_2$ ,

Revision 1

777 whereas that with the highest  $M_r$  is ferro-ferri-cannilloite,  $\text{CaCa}_2(\text{Fe}^{2+}_4\text{Fe}^{3+})(\text{Si}_5\text{Al}_3)\text{O}_{22}(\text{OH})_2$ . Because  
778 of EMP analytical errors, the original amphibole compositions show *TEO* (Total Elements and Oxides)  
779 varying from 98.3 to 100.8 wt%. Underestimated (< 100 wt%) and overestimated (> 100 wt%)  
780 compositions are located above and below the ideal relations, respectively. See the text for additional  
781 details.

782

783 Figure 2.

784 (a) Correlation between the measured (reference)  $^{\text{W}}\text{O}^{2-}$  values and those calculated with equation 3 for  
785 87 amphiboles with  $^{\text{W}}\text{O}^{2-} \leq 2^{\text{C}}\text{Ti}$  (i.e., poorly-oxidized amphiboles); the 1:1 line is reported together  
786 with the standard ( $\sigma_{\text{est}}$ ) and maximum (Max) errors. (b) The best correlation found between the  
787 reference  $^{\text{W}}\text{O}^{2-}$  values and cation composition for all the 114 high-quality amphibole compositions. The  
788 red dashed lines describe the proposed relations; related equations and statistic errors are also reported  
789 in red. See text for additional details.

790 Figure 3.

791 The correlation between *TC* (Total Coefficient) values and those calculated with equation 5 for the 342  
792 calculated compositions (either normalized or deviated) and the 114 original compositions. Normalized  
793 and deviated *TEO* data are also shown. Maximum and minimum uncertainties of the equation are  
794 +0.005 and -0.004.

795 Figure 4.

796 The correlation between the reference  $^{\text{T}}\text{Si}$  (a),  $^{\text{C}}\text{Al}$  (b),  $^{\text{B}}\text{Na}$  (c) and  $^{\text{A}}(\text{Ca} + \text{Na} + \text{K})$  (d) values and those  
797 calculated with the AMFORM spreadsheet for the amphibole compositions used to calibrate the

Revision 1

798 procedure (blue diamonds) and for those used for testing (yellow triangles). The 1:1 lines are reported  
799 in all diagrams (see Table 3 for statistics).

800 Figure 5.

801 Correlations between the reference  ${}^C\text{Al}$ ,  ${}^A(\text{Na} + \text{K} + \text{Ca})$  and  $\text{Fe}^{3+}$  values (from EMP+SREF±SIMS  
802 data) and those calculated solely from the high-quality EMP analysis in our dataset; (a-c): AMFORM;  
803 (d-f): Locock (2014) without  ${}^W\text{O}^{2-}$  estimates; (g-i): Locock (2014) with  ${}^W\text{O}^{2-}$  estimates. The statistics in  
804 diagrams (c), (f), (i) for  $\text{Fe}^{3+}$  refer to the 87 amphiboles with  ${}^W\text{O}^{2-} \leq 2{}^C\text{Ti}$ , whereas all the other  
805 diagrams refer to all the 114 amphiboles of the dataset; max and min errors are the maximum and  
806 minimum (calculated – reference) values. Symbols are reported in (a) and (f). In (c), (f), (i), highly-  
807 oxidized Ca amphiboles ( ${}^W\text{O}^{2-} > 2{}^C\text{Ti}$ ) are distinguished by orange empty squares while yellow squares  
808 are additional Ca and Na-Ca amphiboles (poorly-oxidized;  ${}^W\text{O}^{2-} \leq 2{}^C\text{Ti}$ ) the  $\text{Fe}^{3+}/\text{Fe}_{\text{tot}}$  value of which  
809 was measured using independent techniques (King et al. 2000; Satoh et al. 2004; Bonadiman et al.  
810 2014; Dyar et al. 2016; see AMFORM.xlsx). The 1:1 line is reported in all diagrams.

811 Figure 6.

812 Correlations between the reference  ${}^W\text{O}^{2-}$  and  $\text{Fe}^{3+}$  values and those calculated with the default (a-b) and  
813 the optional (d-e) procedures in AMFORM for the 114 compositions used for calibration and the 23  
814 compositions with  $\text{Fe}^{3+}$  measured by independent techniques. In these diagrams the 1:1 line is also  
815 shown. (c) and (f) report the errors of  $\text{Fe}^{3+}/\text{Fe}_{\text{tot}}$  calculations versus the reference total iron content  
816 (apfu); the line represent the 0 error reference. In (a) and (b), statistics refer only to highly-oxidized Ca  
817 amphiboles (with  ${}^W\text{O}^{2-} > {}^C\text{Ti}$ ) and ferri-kaersutites, symbols have the same color of statistic values; see  
818 Fig. 4c for the statistics of poorly-oxidized amphiboles. In (c), (d), (e) and (f) statistics refer to all the  
819 137 amphiboles considered. See the text for additional explanations.

Fig 1.

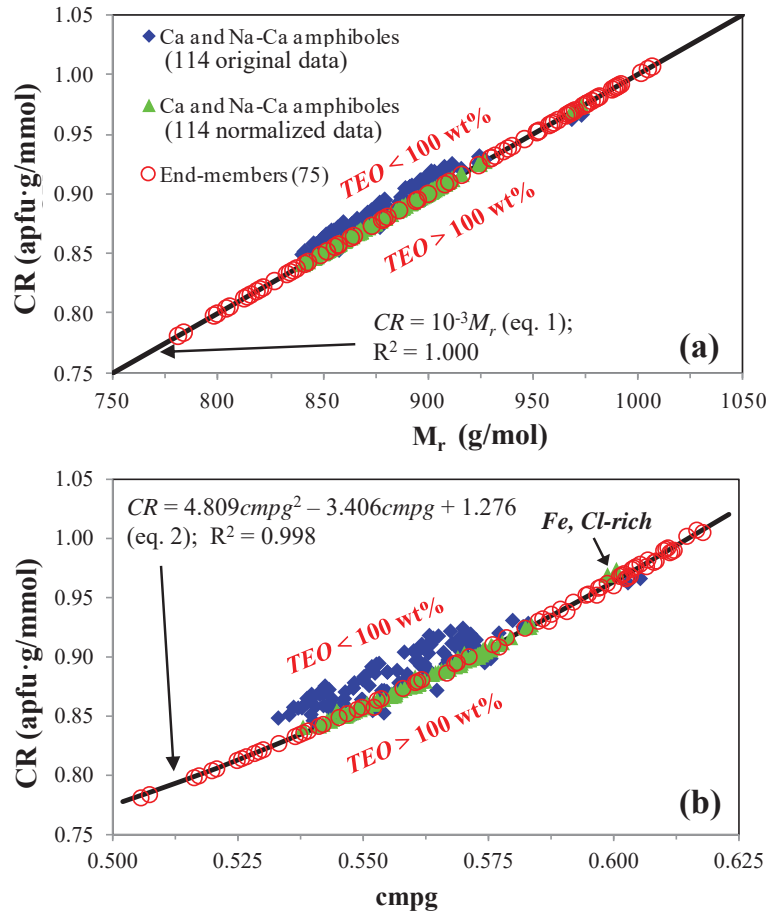


Fig 2.

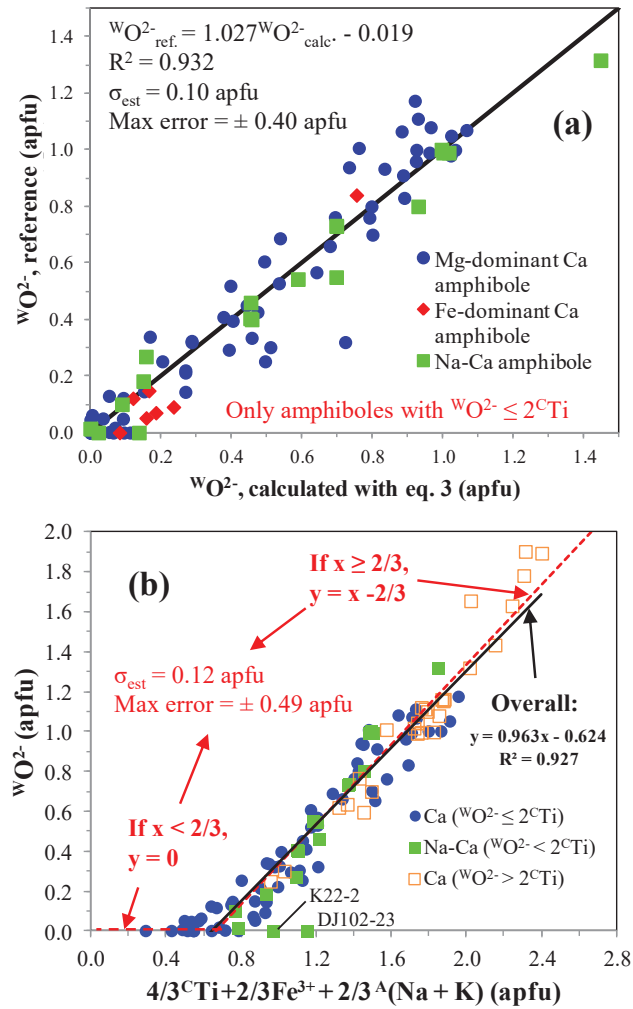


Fig 3.

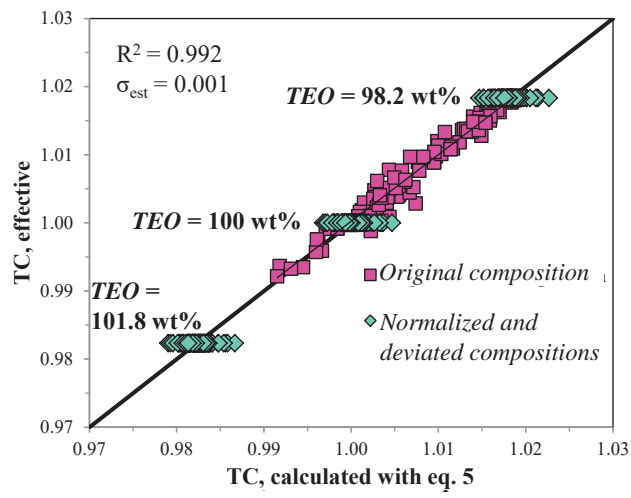




Fig 4.

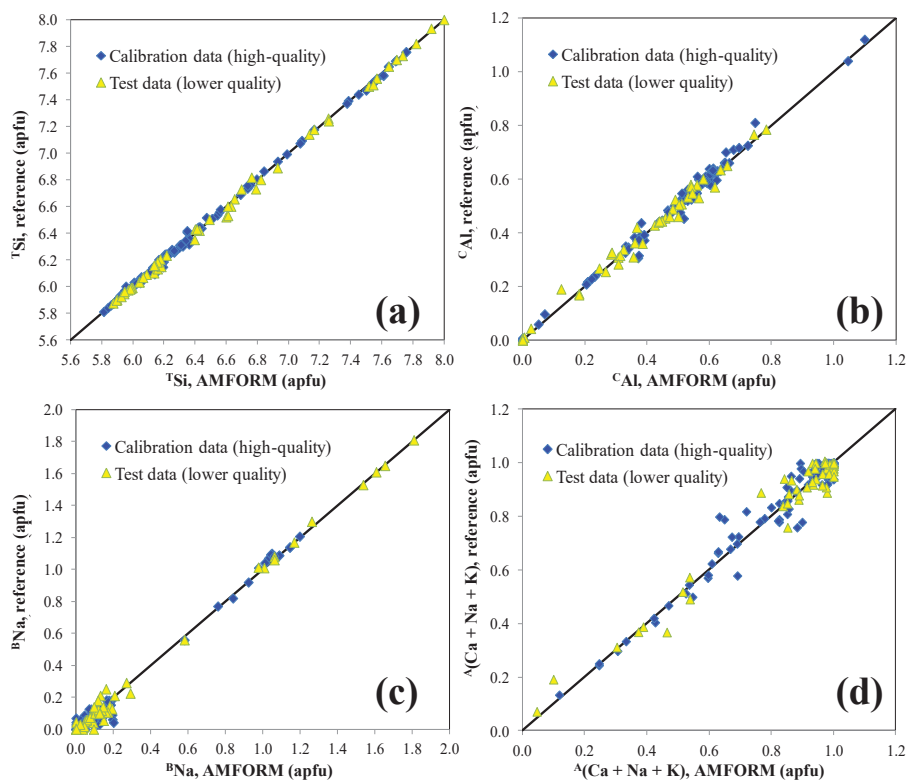


Fig 5.

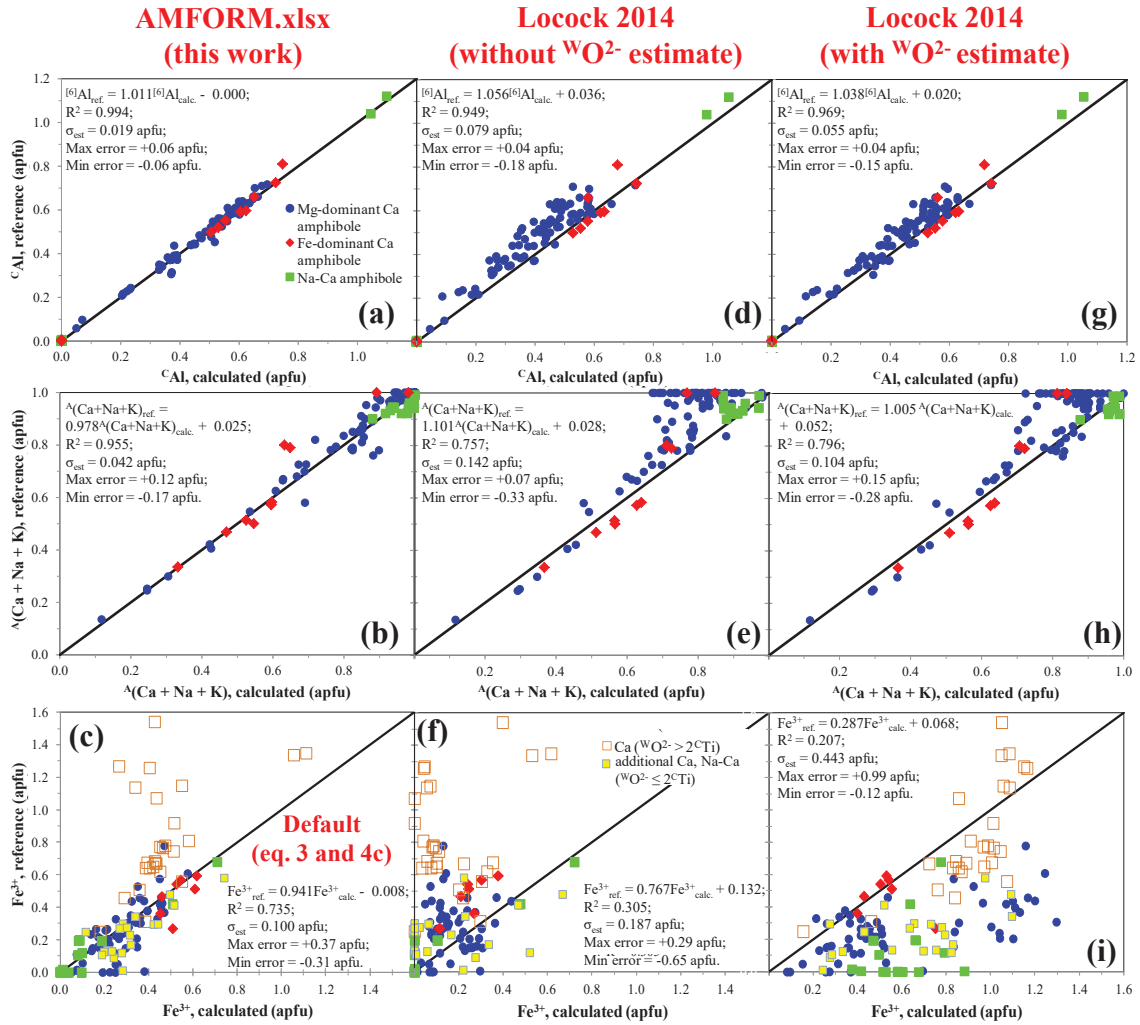


Fig 6.

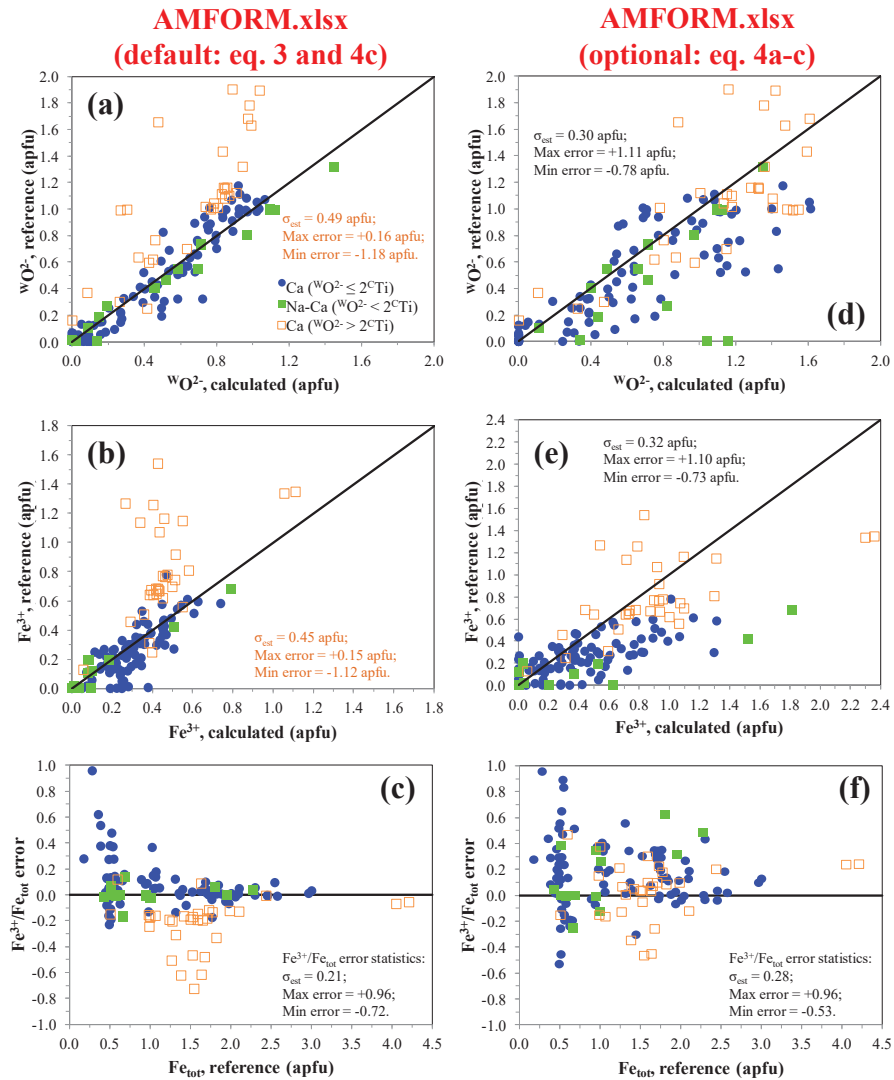


Table 1.

Site-groups and total occupancy		Elements	Stoichiometric constraints (apfu)
Cations (15-16 apfu)			
T (8 apfu)		Si	$Si \leq 8$
		Al	
		Ti	$\sum Si \rightarrow Ti \geq 8$
		Cr	
		Ni	
B (2 apfu)	C (5 apfu)	Zn	
		Fe <sub>tot</sub>	
		Mn	
		Mg	$\sum Si \rightarrow Mg \geq 13$
		Ca	
	A (0-1 apfu)	Na	
		K	$15 \leq \sum Si \rightarrow K \leq 16$
Anions (24 apfu)			
O (22 apfu)		O	$\sum O \geq 22$
		OH	
		F	
		Cl	
	W (2 apfu)		

apfu: atoms per formula units;  $\Delta C = \sum Si \rightarrow Mg - 13$  (Mn, Fe<sup>2+</sup> and Mg occurring as B cations). Notes: Fe<sub>tot</sub> = Fe<sup>3+</sup> + Fe<sup>2+</sup> (only Fe<sup>2+</sup> is assigned to the B sites)

Table 2.

Name	Group	Sub-group	Formula	SiO <sub>2</sub>	TiO <sub>2</sub>	Al <sub>2</sub> O <sub>3</sub>	FeO <sub>tot</sub>	MgO	CaO	Na <sub>2</sub> O	Sum	Fe <sub>2</sub> O <sub>3</sub>	FeO	H <sub>2</sub> O	M <sub>r</sub>	cmprg
Cummingtonite	<sup>W</sup> (OH,F,Cl)	Mg-Fe-Mn	□Mg <sub>5</sub> Mg <sub>3</sub> Si <sub>8</sub> O <sub>22</sub> (OH) <sub>2</sub>	61.56	0.00	0.00	0.00	36.13	0.00	0.00	97.69			2.31	781	0.506
Glucophane	<sup>W</sup> (OH,F,Cl)	Na	□Na <sub>2</sub> (Mg <sub>3</sub> Al <sub>2</sub> )Si <sub>8</sub> O <sub>22</sub> (OH) <sub>2</sub>	61.35	0.00	13.01	0.00	15.43	0.00	7.91	97.70			2.30	784	0.507
Winchite	<sup>W</sup> (OH,F,Cl)	Na-Ca	□(NaCa)(Mg <sub>5</sub> Al)Si <sub>8</sub> O <sub>22</sub> (OH) <sub>2</sub>	60.24	0.00	6.39	0.00	20.20	7.03	3.88	97.74			2.26	798	0.516
Barroisite	<sup>W</sup> (OH,F,Cl)	Na-Ca	□(NaCa)(Mg <sub>4</sub> Al <sub>2</sub> )(Si <sub>7</sub> Al)O <sub>22</sub> (OH) <sub>2</sub>	52.60	0.00	19.13	0.00	15.12	7.01	3.88	97.75			2.25	800	0.517
Eckermannite	<sup>W</sup> (OH,F,Cl)	Na	NaNa <sub>2</sub> (Mg <sub>4</sub> Al)Si <sub>8</sub> O <sub>22</sub> (OH) <sub>2</sub>	59.80	0.00	6.34	0.00	20.06	0.00	11.57	97.76			2.24	804	0.520
Nyboite	<sup>W</sup> (OH,F,Cl)	Na	NaNa <sub>2</sub> (Mg <sub>3</sub> Al <sub>2</sub> )(Si <sub>7</sub> Al)O <sub>22</sub> (OH) <sub>2</sub>	52.22	0.00	18.99	0.00	15.01	0.00	11.54	97.76			2.24	805	0.521
Tremolite	<sup>W</sup> (OH,F,Cl)	Ca	□Ca <sub>2</sub> Mg <sub>5</sub> Si <sub>8</sub> O <sub>22</sub> (OH) <sub>2</sub>	59.17	0.00	0.00	0.00	24.81	13.81	0.00	97.78			2.22	812	0.525
Magnesio-hornblende	<sup>W</sup> (OH,F,Cl)	Ca	□Ca <sub>2</sub> (Mg <sub>4</sub> Al)(Si <sub>7</sub> Al)O <sub>22</sub> (OH) <sub>2</sub>	51.67	0.00	12.53	0.00	19.81	13.78	0.00	97.79			2.21	814	0.526
Tschermakite	<sup>W</sup> (OH,F,Cl)	Ca	□Ca <sub>2</sub> (Mg <sub>3</sub> Al <sub>2</sub> )(Si <sub>6</sub> Al <sub>2</sub> )O <sub>22</sub> (OH) <sub>2</sub>	44.21	0.00	25.01	0.00	14.83	13.75	0.00	97.79			2.21	815	0.527
Richterite	<sup>W</sup> (OH,F,Cl)	Na-Ca	Na(NaCa)Mg <sub>5</sub> Si <sub>8</sub> O <sub>22</sub> (OH) <sub>2</sub>	58.74	0.00	0.00	0.00	24.63	6.85	7.57	97.80			2.20	818	0.528
Katophorite	<sup>W</sup> (OH,F,Cl)	Na-Ca	Na(NaCa)(Mg <sub>4</sub> Al)(Si <sub>7</sub> Al)O <sub>22</sub> (OH) <sub>2</sub>	51.30	0.00	12.44	0.00	19.66	6.84	7.56	97.80			2.20	820	0.529
Taramite	<sup>W</sup> (OH,F,Cl)	Na-Ca	Na(NaCa)(Mg <sub>3</sub> Al <sub>2</sub> )(Si <sub>6</sub> Al <sub>2</sub> )O <sub>22</sub> (OH) <sub>2</sub>	43.89	0.00	24.83	0.00	14.72	6.83	7.55	97.81			2.19	821	0.530
Ferri-winchite	<sup>W</sup> (OH,F,Cl)	Na-Ca	□(NaCa)(Mg <sub>4</sub> Fe <sup>3+</sup> )Si <sub>8</sub> O <sub>22</sub> (OH) <sub>2</sub>	58.14	0.00	6.01	8.69	19.50	6.78	3.75	96.85	9.66	0.00	2.18	825	0.533
Magnesio-arfvedsonite	<sup>W</sup> (OH,F,Cl)	Na	NaNa <sub>2</sub> (Mg <sub>4</sub> Fe <sup>3+</sup> )Si <sub>8</sub> O <sub>22</sub> (OH) <sub>2</sub>	57.72	0.00	0.00	8.63	19.36	0.00	11.16	96.88	9.59	0.00	2.16	833	0.536
Edenite	<sup>W</sup> (OH,F,Cl)	Ca	NaCa <sub>2</sub> Mg <sub>3</sub> (Si <sub>7</sub> Al)O <sub>22</sub> (OH) <sub>2</sub>	50.41	0.00	6.11	0.00	24.16	13.44	3.71	97.84			2.16	834	0.537
Pargasite	<sup>W</sup> (OH,F,Cl)	Ca	NaCa <sub>2</sub> (Mg <sub>4</sub> Al)(Si <sub>6</sub> Al <sub>2</sub> )O <sub>22</sub> (OH) <sub>2</sub>	43.13	0.00	18.30	0.00	19.29	13.42	3.71	97.84			2.16	836	0.538
Sadanagaite	<sup>W</sup> (OH,F,Cl)	Ca	NaCa <sub>2</sub> (Mg <sub>3</sub> Al <sub>2</sub> )(Si <sub>6</sub> Al <sub>2</sub> )O <sub>22</sub> (OH) <sub>2</sub>	35.88	0.00	30.44	0.00	14.44	13.39	3.70	97.85			2.15	837	0.539
Magnesio-riebeckite	<sup>W</sup> (OH,F,Cl)	Na	□Na <sub>2</sub> (Mg <sub>3</sub> Fe <sup>3+</sup> )Si <sub>8</sub> O <sub>22</sub> (OH) <sub>2</sub>	57.14	0.00	0.00	17.08	14.37	0.00	7.37	95.96	18.98	0.00	2.14	841	0.541
Magnesio-ferri-hornblende	<sup>W</sup> (OH,F,Cl)	Ca	□Ca <sub>2</sub> (Mg <sub>4</sub> Fe <sup>3+</sup> )(Si <sub>7</sub> Al)O <sub>22</sub> (OH) <sub>2</sub>	49.90	0.00	6.05	8.52	19.13	13.31	0.00	96.91	9.47	0.00	2.14	843	0.542
Ferri-katophorite	<sup>W</sup> (OH,F,Cl)	Na-Ca	Na(NaCa)(Mg <sub>4</sub> Fe <sup>3+</sup> )(Si <sub>7</sub> Al)O <sub>22</sub> (OH) <sub>2</sub>	49.56	0.00	6.01	8.47	19.00	6.61	7.30	96.93	9.41	0.00	2.12	849	0.545
Cannilloite	<sup>W</sup> (OH,F,Cl)	Ca	CaCa <sub>2</sub> (Mg <sub>4</sub> Al)(Si <sub>6</sub> Al <sub>2</sub> )O <sub>22</sub> (OH) <sub>2</sub>	35.27	0.00	23.94	0.00	18.93	19.75	0.00	97.89			2.11	852	0.547
Rootname 4	<sup>W</sup> (OH,F,Cl)	Ca	NaCa <sub>2</sub> (Mg <sub>4</sub> Ti)(Si <sub>6</sub> Al <sub>2</sub> )O <sub>22</sub> (OH) <sub>2</sub>	35.11	9.33	17.88	0.00	18.84	13.11	3.62	97.89			2.11	856	0.549
Kaersutite	<sup>W</sup> O	-	NaCa <sub>2</sub> (Mg <sub>3</sub> TiAl)(Si <sub>6</sub> Al <sub>2</sub> )O <sub>22</sub> O <sub>2</sub>	42.05	9.32	17.84	0.00	14.10	13.08	3.61	100.00			0.00	857	0.552
Ferri-barroisite	<sup>W</sup> (OH,F,Cl)	Na-Ca	Na(NaCa)(Mg <sub>3</sub> Fe <sup>3+</sup> )(Si <sub>7</sub> Al)O <sub>22</sub> (OH) <sub>2</sub>	49.06	0.00	5.95	16.76	14.10	6.54	3.61	96.03	18.63	0.00	2.10	857	0.550
Ferri-nyboite	<sup>W</sup> (OH,F,Cl)	Na	NaNa <sub>2</sub> (Mg <sub>3</sub> Fe <sup>3+</sup> )(Si <sub>7</sub> Al)O <sub>22</sub> (OH) <sub>2</sub>	48.73	0.00	5.91	16.65	14.01	0.00	10.77	96.06	18.50	0.00	2.09	863	0.553
Magnesio-hastingsite	<sup>W</sup> (OH,F,Cl)	Ca	NaCa <sub>2</sub> (Mg <sub>3</sub> Fe <sup>3+</sup> )(Si <sub>6</sub> Al <sub>2</sub> )O <sub>22</sub> (OH) <sub>2</sub>	41.69	0.00	11.79	8.31	18.64	12.97	3.58	96.99	9.23	0.00	2.08	865	0.554
Ferri-tschermakite	<sup>W</sup> (OH,F,Cl)	Ca	□Ca <sub>2</sub> (Mg <sub>3</sub> Fe <sup>3+</sup> )(Si <sub>6</sub> Al <sub>2</sub> )O <sub>22</sub> (OH) <sub>2</sub>	41.28	0.00	11.68	16.45	13.85	12.84	0.00	96.10	18.29	0.00	2.06	873	0.558
Ferro-glucophane	<sup>W</sup> (OH,F,Cl)	Na	□Na <sub>2</sub> (Fe <sup>2+</sup> <sub>3</sub> Al <sub>2</sub> )Si <sub>8</sub> O <sub>22</sub> (OH) <sub>2</sub>	54.74	0.00	11.61	24.54	0.00	0.00	7.06	97.95	0.00	24.54	2.05	878	0.560
Ferri-taramite	<sup>W</sup> (OH,F,Cl)	Na-Ca	Na(NaCa)(Mg <sub>3</sub> Fe <sup>3+</sup> )(Si <sub>6</sub> Al <sub>2</sub> )O <sub>22</sub> (OH) <sub>2</sub>	41.01	0.00	11.60	16.34	13.75	6.38	7.05	96.13	18.16	0.00	2.05	879	0.561
Ferri-cannilloite	<sup>W</sup> (OH,F,Cl)	Ca	CaCa <sub>2</sub> (Mg <sub>4</sub> Fe <sup>3+</sup> )(Si <sub>6</sub> Al <sub>2</sub> )O <sub>22</sub> (OH) <sub>2</sub>	34.11	0.00	17.37	8.16	18.31	19.10	0.00	97.05	9.07	0.00	2.05	881	0.562
Ferri-kaersutite	<sup>W</sup> O	-	NaCa <sub>2</sub> (Mg <sub>3</sub> TiFe <sup>3+</sup> )(Si <sub>6</sub> Al <sub>2</sub> )O <sub>22</sub> O <sub>2</sub>	40.68	9.01	11.51	8.11	13.64	12.66	3.50	99.10	9.01	0.00	0.00	886	0.567
Ferro-barroisite	<sup>W</sup> (OH,F,Cl)	Na-Ca	□(NaCa)(Fe <sup>2+</sup> <sub>3</sub> Al <sub>2</sub> )(Si <sub>7</sub> Al)O <sub>22</sub> (OH) <sub>2</sub>	47.04	0.00	17.10	24.11	0.00	6.27	3.47	97.99	0.00	24.11	2.01	894	0.568
Ferri-sadanagaite	<sup>W</sup> (OH,F,Cl)	Ca	NaCa <sub>2</sub> (Mg <sub>3</sub> Fe <sup>3+</sup> )(Si <sub>6</sub> Al <sub>2</sub> )O <sub>22</sub> (OH) <sub>2</sub>	33.56	0.00	17.09	16.05	13.51	12.53	3.46	96.20	17.84	0.00	2.01	895	0.569
Ferro-nyboite	<sup>W</sup> (OH,F,Cl)	Na	NaNa <sub>2</sub> (Fe <sup>2+</sup> <sub>3</sub> Al <sub>2</sub> )(Si <sub>7</sub> Al)O <sub>22</sub> (OH) <sub>2</sub>	46.73	0.00	16.99	23.95	0.00	0.00	10.33	98.00	0.00	23.95	2.00	900	0.571
oxo Ferro-tschermakite	<sup>W</sup> O	Ca	□Ca <sub>2</sub> (Fe <sup>2+</sup> <sub>2</sub> Fe <sup>3+</sup> <sub>2</sub> Al <sub>2</sub> )(Si <sub>6</sub> Al <sub>2</sub> )O <sub>22</sub> O <sub>2</sub>	39.70	0.00	22.46	23.73	0.00	12.35	0.00	98.24	17.58	7.91	0.00	908	0.577
Ferro-tschermakite	<sup>W</sup> (OH,F,Cl)	Ca	□Ca <sub>2</sub> (Fe <sup>2+</sup> <sub>3</sub> Al <sub>2</sub> )(Si <sub>6</sub> Al <sub>2</sub> )O <sub>22</sub> (OH) <sub>2</sub>	39.61	0.00	22.41	23.68	0.00	12.32	0.00	98.02	0.00	23.68	1.98	910	0.576
Ferro-taramite	<sup>W</sup> (OH,F,Cl)	Na-Ca	Na(NaCa)(Fe <sup>2+</sup> <sub>3</sub> Al <sub>2</sub> )(Si <sub>6</sub> Al <sub>2</sub> )O <sub>22</sub> (OH) <sub>2</sub>	39.35	0.00	22.26	23.53	0.00	6.12	6.77	98.03	0.00	23.53	1.97	916	0.579
Ferro-winchite	<sup>W</sup> (OH,F,Cl)	Na-Ca	□(NaCa)(Fe <sup>2+</sup> +4Al)Si <sub>8</sub> O <sub>22</sub> (OH) <sub>2</sub>	52.01	0.00	5.52	31.10	0.00	6.07	3.35	98.05	0.00	31.10	1.95	924	0.582
oxo Ferro-sadanagaite	<sup>W</sup> O	Ca	NaCa <sub>2</sub> (Fe <sup>2+</sup> <sub>3</sub> Fe <sup>3+</sup> <sub>2</sub> Al <sub>2</sub> )(Si <sub>6</sub> Al <sub>2</sub> )O <sub>22</sub> O <sub>2</sub>	32.30	0.00	27.41	23.18	0.00	12.06	3.33	98.28	17.17	7.73	0.00	930	0.587
Ferro-eckermannite	<sup>W</sup> (OH,F,Cl)	Na	NaNa <sub>2</sub> (Fe <sup>2+</sup> <sub>4</sub> Al)Si <sub>8</sub> O <sub>22</sub> (OH) <sub>2</sub>	51.68	0.00	5.48	30.90	0.00	0.00	10.00	98.06	0.00	30.90	1.94	930	0.585
Ferro-sadanagaite	<sup>W</sup> (OH,F,Cl)	Ca	NaCa <sub>2</sub> (Fe <sup>2+</sup> <sub>3</sub> Al <sub>2</sub> )(Si <sub>6</sub> Al <sub>2</sub> )O <sub>22</sub> (OH) <sub>2</sub>	32.23	0.00	27.35	23.13	0.00	12.03	3.33	98.07	0.00	23.13	1.93	932	0.586
Riebeckite	<sup>W</sup> (OH,F,Cl)	Na	□Na <sub>2</sub> (Fe <sup>2+</sup> <sub>3</sub> Fe <sup>3+</sup> <sub>2</sub> )Si <sub>8</sub> O <sub>22</sub> (OH) <sub>2</sub>	51.36	0.00	0.00	38.38	0.00	0.00	6.62	96.37	17.06	23.03	1.92	936	0.588
oxo Ferro-hornblende	<sup>W</sup> O	Ca	□Ca <sub>2</sub> (Fe <sup>2+</sup> <sub>2</sub> Fe <sup>3+</sup> <sub>2</sub> Al)(Si <sub>7</sub> Al)O <sub>22</sub> O <sub>2</sub>	44.83	0.00	10.87	30.63	0.00	11.96	0.00	98.29	17.02	15.32	0.00	938	0.591
Ferro-hornblende	<sup>W</sup> (OH,F,Cl)	Ca	□Ca <sub>2</sub> (Fe <sup>2+</sup> <sub>4</sub> Al)(Si <sub>7</sub> Al)O <sub>22</sub> (OH) <sub>2</sub>	44.74	0.00	10.85	30.57	0.00	11.93	0.00	98.08	0.00	30.57	1.92	940	0.589
Ferro-katophorite	<sup>W</sup> (OH,F,Cl)	Na-Ca	Na(NaCa)(Fe <sup>2+</sup> <sub>4</sub> Al)(Si <sub>7</sub> Al)O <sub>22</sub> (OH) <sub>2</sub>	44.46	0.00	10.78	30.38	0.00	5.93	6.55	98.10	0.00	30.38	1.90	946	0.592
Ferro-ferri-barroisite	<sup>W</sup> (OH,F,Cl)	Na-Ca	□(NaCa)(Fe <sup>2+</sup> <sub>3</sub> Fe <sup>3+</sup> <sub>2</sub> )(Si <sub>7</sub> Al)O <sub>22</sub> (OH) <sub>2</sub>	44.19	0.00	5.36	37.74	0.00	5.89	3.26	96.43	16.78	22.64	1.89	952	0.594
Ferro-kaersutite	<sup>W</sup> O	-	NaCa <sub>2</sub> (Fe <sup>2+</sup> <sub>3</sub> TiAl)(Si <sub>6</sub> Al <sub>2</sub> )O <sub>22</sub> O <sub>2</sub>	37.87	8.39	16.07	22.64	0.00	11.78	3.26	100.00	0.00	22.64	0.00	952	0.597
Ferro-ferri-winchite	<sup>W</sup> (OH,F,Cl)	Na-Ca	□(NaCa)(Fe <sup>2+</sup> <sub>4</sub> Fe <sup>3+</sup> )Si <sub>8</sub> O <sub>22</sub> (OH) <sub>2</sub>	50.44	0.00	0.00	37.69	0.00	5.88	3.25	97.27	8.38	30.16	1.89	953	0.595
Ferro-ferri-nyboite	<sup>W</sup> (OH,F,Cl)	Na	NaNa <sub>2</sub> (Fe <sup>2+</sup> +3Fe <sup>3+</sup> +2)(Si <sub>7</sub> Al)O <sub>22</sub> (OH) <sub>2</sub>	43.91	0.00	5.32	37.51	0.00	0.00	9.71	96.45	16.67	22.50	1.88	958	0.597
Arfvedsonite	<sup>W</sup> (OH,F,Cl)	Na	NaNa <sub>2</sub> (Fe <sup>2+</sup> <sub>4</sub> Fe <sup>3+</sup> )Si <sub>8</sub> O <sub>22</sub> (OH) <sub>2</sub>	50.13	0.00	0.00	37.46	0.00	0.00	9.70	97.29	8.33	29.97	1.88	959	0.597
oxo Ferro-pargasite	<sup>W</sup> O	Ca	NaCa <sub>2</sub> (Fe <sup>2+</sup> <sub>2</sub> Fe <sup>3+</sup> <sub>2</sub> Al)(Si <sub>6</sub> Al <sub>2</sub> )O <sub>22</sub> O <sub>2</sub>	37.55	0.00	15.93	29.94	0.00	11.68	3.23	98.33	16.63	14.97	0.00	960	0.600
Ferro-pargasite	<sup>W</sup> (OH,F,Cl)	Ca	NaCa <sub>2</sub> (Fe <sup>2+</sup> <sub>4</sub> Al)(Si <sub>6</sub> Al <sub>2</sub> )O <sub>22</sub> (OH) <sub>2</sub>	37.47	0.00	15.90	29.8									

Table 2. Continue.

Name	Group	Sub-group	Formula	SiO <sub>2</sub>	TiO <sub>2</sub>	Al <sub>2</sub> O <sub>3</sub>	FeO <sub>tot</sub>	MgO	CaO	Na <sub>2</sub> O	Sum	Fe <sub>2</sub> O <sub>3</sub>	FeO	H <sub>2</sub> O	M <sub>r</sub>	cmpg
oxo Ferro-fërri-hornblende	<sup>W</sup> O	Ca	□Ca <sub>2</sub> (Fe <sup>2+</sup> <sub>2</sub> Fe <sup>3+</sup> <sub>3</sub> )(Si <sub>7</sub> Al)O <sub>22</sub> O <sub>2</sub>	43.50	0.00	5.27	37.15	0.00	11.60	0.00	97.52	24.77	14.86	0.00	967	0.603
oxo Ferro-cannilloite	<sup>W</sup> O	Ca	CaCa <sub>2</sub> (Fe <sup>2+</sup> <sub>2</sub> Fe <sup>3+</sup> <sub>2</sub> Al)(Si <sub>5</sub> Al <sub>3</sub> )O <sub>22</sub> O <sub>2</sub>	30.78	0.00	20.89	29.45	0.00	17.24	0.00	98.36	16.36	14.72	0.00	976	0.607
oxo Ferro-fërri-tschermakite	<sup>W</sup> O	Ca	□Ca <sub>2</sub> (Fe <sup>2+</sup> <sub>2</sub> Fe <sup>3+</sup> <sub>4</sub> )(Si <sub>6</sub> Al <sub>2</sub> )O <sub>22</sub> O <sub>2</sub>	37.33	0.00	10.56	37.19	0.00	11.61	0.00	96.69	33.07	7.44	0.00	966	0.602
Ferro-fërri-tschermakite	<sup>W</sup> (OH,F,Cl)	Ca	□Ca <sub>2</sub> (Fe <sup>2+</sup> <sub>3</sub> Fe <sup>3+</sup> <sub>2</sub> )(Si <sub>6</sub> Al <sub>2</sub> )O <sub>22</sub> (OH) <sub>2</sub>	37.25	0.00	10.53	37.12	0.00	11.59	0.00	96.49	16.50	22.27	1.86	968	0.601
oxo Ferro-actinolite	<sup>W</sup> O	Ca	□Ca <sub>2</sub> (Fe <sup>2+</sup> <sub>3</sub> Fe <sup>3+</sup> <sub>2</sub> )Si <sub>8</sub> O <sub>22</sub> O <sub>2</sub>	49.65	0.00	0.00	37.11	0.00	11.59	0.00	98.35	16.50	22.26	0.00	968	0.603
Ferro-fërri-hornblende	<sup>W</sup> (OH,F,Cl)	Ca	□Ca <sub>2</sub> (Fe <sup>2+</sup> <sub>4</sub> Fe <sup>3+</sup> <sub>3</sub> )(Si <sub>7</sub> Al)O <sub>22</sub> (OH) <sub>2</sub>	43.41	0.00	5.26	37.07	0.00	11.57	0.00	97.32	8.24	29.66	1.86	969	0.602
Ferro-actinolite	<sup>W</sup> (OH,F,Cl)	Ca	□Ca <sub>2</sub> Fe <sup>2+</sup> <sub>5</sub> Si <sub>8</sub> O <sub>22</sub> (OH) <sub>2</sub>	49.55	0.00	0.00	37.03	0.00	11.56	0.00	98.14	0.00	37.03	1.86	970	0.602
Ferro-fërri-taramite	<sup>W</sup> (OH,F,Cl)	Na-Ca	Na(NaCa)(Fe <sup>2+</sup> <sub>3</sub> Fe <sup>3+</sup> <sub>2</sub> )(Si <sub>6</sub> Al <sub>3</sub> )O <sub>22</sub> (OH) <sub>2</sub>	37.02	0.00	10.47	36.89	0.00	5.76	6.36	96.51	16.40	22.13	1.85	974	0.604
Ferro-fërri-katophorite	<sup>W</sup> (OH,F,Cl)	Na-Ca	Na(NaCa)(Fe <sup>2+</sup> <sub>4</sub> Fe <sup>3+</sup> <sub>3</sub> )(Si <sub>7</sub> Al)O <sub>22</sub> (OH) <sub>2</sub>	43.14	0.00	5.23	36.85	0.00	5.75	6.36	97.33	8.19	29.48	1.85	975	0.604
Ferro-richterite	<sup>W</sup> (OH,F,Cl)	Na-Ca	Na(NaCa)Fe <sup>2+</sup> <sub>5</sub> Si <sub>8</sub> O <sub>22</sub> (OH) <sub>2</sub>	49.25	0.00	0.00	36.81	0.00	5.75	6.35	98.15	0.00	36.81	1.85	976	0.604
Ferro-cannilloite	<sup>W</sup> (OH,F,Cl)	Ca	CaCa <sub>2</sub> (Fe <sup>2+</sup> <sub>4</sub> Al)(Si <sub>5</sub> Al <sub>3</sub> )O <sub>22</sub> (OH) <sub>2</sub>	30.72	0.00	20.85	29.39	0.00	17.20	0.00	98.16	0.00	29.39	1.84	978	0.605
oxo Ferro-rootname 4	<sup>W</sup> O	Ca	NaCa <sub>2</sub> (Fe <sup>2+</sup> <sub>2</sub> Fe <sup>3+</sup> <sub>2</sub> Ti)(Si <sub>5</sub> Al <sub>3</sub> )O <sub>22</sub> O <sub>2</sub>	30.66	8.15	15.61	29.33	0.00	11.45	3.16	98.37	16.30	14.67	0.00	980	0.608
Ferro-fërri-kaersutite	<sup>W</sup> O	-	NaCa <sub>2</sub> (Fe <sup>2+</sup> <sub>3</sub> TiFe <sup>3+</sup> <sub>3</sub> )(Si <sub>6</sub> Al <sub>2</sub> )O <sub>22</sub> O <sub>2</sub>	36.75	8.14	10.40	29.30	0.00	11.43	3.16	99.18	8.14	21.97	0.00	981	0.609
Ferro-rootname 4	<sup>W</sup> (OH,F,Cl)	Ca	NaCa <sub>2</sub> (Fe <sup>2+</sup> <sub>4</sub> Ti)(Si <sub>5</sub> Al <sub>3</sub> )O <sub>22</sub> (OH) <sub>2</sub>	30.60	8.13	15.58	29.27	0.00	11.42	3.16	98.17	0.00	29.27	1.83	982	0.607
oxo Ferro-fërri-sadanagaite	<sup>W</sup> O	Ca	NaCa <sub>2</sub> (Fe <sup>2+</sup> <sub>3</sub> Fe <sup>3+</sup> <sub>4</sub> )(Si <sub>6</sub> Al <sub>3</sub> )O <sub>22</sub> O <sub>2</sub>	30.42	0.00	15.48	36.37	0.00	11.35	3.14	96.76	32.33	7.27	0.00	988	0.611
oxo Hastingsite	<sup>W</sup> O	Ca	NaCa <sub>2</sub> (Fe <sup>2+</sup> <sub>2</sub> Fe <sup>3+</sup> <sub>3</sub> )(Si <sub>6</sub> Al <sub>2</sub> )O <sub>22</sub> O <sub>2</sub>	36.46	0.00	10.31	36.33	0.00	11.34	3.13	97.57	24.22	14.53	0.00	989	0.612
Ferro-fërri-sadanagaite	<sup>W</sup> (OH,F,Cl)	Ca	NaCa <sub>2</sub> (Fe <sup>2+</sup> <sub>3</sub> Fe <sup>3+</sup> <sub>2</sub> )(Si <sub>5</sub> Al <sub>3</sub> )O <sub>22</sub> (OH) <sub>2</sub>	30.35	0.00	15.45	36.29	0.00	11.33	3.13	96.56	16.13	21.78	1.82	990	0.610
oxo Ferro-edenite	<sup>W</sup> O	Ca	NaCa <sub>2</sub> (Fe <sup>2+</sup> <sub>3</sub> Fe <sup>3+</sup> <sub>2</sub> )(Si <sub>7</sub> Al)O <sub>22</sub> O <sub>2</sub>	42.49	0.00	5.15	36.29	0.00	11.33	3.13	98.38	16.13	21.77	0.00	990	0.612
Hastingsite	<sup>W</sup> (OH,F,Cl)	Ca	NaCa <sub>2</sub> (Fe <sup>2+</sup> <sub>4</sub> Fe <sup>3+</sup> <sub>3</sub> )(Si <sub>6</sub> Al <sub>2</sub> )O <sub>22</sub> (OH) <sub>2</sub>	36.38	0.00	10.29	36.25	0.00	11.32	3.13	97.37	8.06	29.00	1.82	991	0.610
Ferro-edenite	<sup>W</sup> (OH,F,Cl)	Ca	NaCa <sub>2</sub> Fe <sup>2+</sup> <sub>5</sub> (Si <sub>7</sub> Al)O <sub>22</sub> (OH) <sub>2</sub>	42.40	0.00	5.14	36.21	0.00	11.31	3.12	98.18	0.00	36.21	1.82	992	0.611
Grunerite	<sup>W</sup> (OH,F,Cl)	Mg-Fe-Mn	□Fe <sup>2+</sup> <sub>2</sub> Fe <sup>2+</sup> <sub>3</sub> Si <sub>8</sub> O <sub>22</sub> (OH) <sub>2</sub>	47.99	0.00	0.00	50.21	0.00	0.00	0.00	98.20	0.00	50.21	1.80	1002	0.615
oxo Ferro-fërri-cannilloite	<sup>W</sup> O	Ca	CaCa <sub>2</sub> (Fe <sup>2+</sup> <sub>2</sub> Fe <sup>3+</sup> <sub>3</sub> )(Si <sub>5</sub> Al <sub>3</sub> )O <sub>22</sub> O <sub>2</sub>	29.90	0.00	15.22	35.75	0.00	16.74	0.00	97.61	23.84	14.30	0.00	1005	0.618
Ferro-fërri-cannilloite	<sup>W</sup> (OH,F,Cl)	Ca	CaCa <sub>2</sub> (Fe <sup>2+</sup> <sub>4</sub> Fe <sup>3+</sup> <sub>3</sub> )(Si <sub>6</sub> Al <sub>2</sub> )O <sub>22</sub> (OH) <sub>2</sub>	29.84	0.00	15.19	35.68	0.00	16.71	0.00	97.42	7.93	28.54	1.79	1007	0.617

Table 3.

Amphibole parameter	Calibration high-quality data N = 114		Test lower-quality data N = 51	
	$\sigma_{\text{est}}$	max error	$\sigma_{\text{est}}$	max error
<sup>T</sup> Si	0.017	0.068	0.026	0.081
Ti	0.002	0.008	0.002	0.006
Al <sub>tot</sub>	0.006	0.018	0.021	0.077
Fe <sub>tot</sub>	0.007	0.045	0.024	0.121
Mg	0.008	0.028	0.015	0.045
Ca	0.005	0.019	0.005	0.016
Na	0.003	0.010	0.006	0.035
K	0.002	0.007	0.002	0.005
F	0.004	0.016	0.013	0.060
<sup>C</sup> Ti	0.012 (0.017)	0.087	0.007 (0.026)	0.039
<sup>C</sup> Al	0.019 (0.018)	0.065	0.023 (0.034)	0.066
$\Delta C$	0.035 (0.021)	0.140	0.035 (0.044)	0.101
<sup>B</sup> Na	0.036 (0.022)	0.159	0.036 (0.044)	0.095
<sup>A</sup> (Ca + Na + K)	0.042 (0.022)	0.168	0.044 (0.045)	0.124
Fe <sup>3+</sup> , default*	0.100 (0.126)	0.373	0.151 (0.169)	0.620
Fe <sup>3+</sup> , optional	0.303 (0.248)	1.104	0.361 (0.419)	1.001
$\Delta\text{MM}\%$	0.18	0.74	0.29	0.87

N: sample number;  $\sigma_{\text{est}}$ : standard error of the estimate; max error: maximum error;

\*: N = 87 and 40 for calibration quality and test data (only amphiboles with  $^{\text{W}}\text{O}^{2-} \leq 2^{\text{C}}\text{Ti}$ );

brackets report errors due to the uncertainty propagation in the calculation of the parameters.